Kotsifaki, R., Sideris, V., King, E., Bahr, R., Whiteley, R. (2023). Performance and symmetry measures during vertical jump testing at return to sport after ACL reconstruction. *British Journal of Sports Medicine*. http://dx.doi.org/10.1136/bjsports-2022-106588

Performance and symmetry measures during vertical jump testing at return to sport after ACL reconstruction

Authors:

Roula Kotsifaki[1,2], Vasileios Sideris[1], Enda King[1,3], Roald Bahr[2,4], Rodney Whiteley[1,5]

Affiliations:

1. Rehabilitation Department, Aspetar, Orthopaedic and Sports Medicine Hospital, Doha, Qatar
2. Oslo Sports Trauma Research Center, Department of Sports Medicine, Norwegian School of Sport Sciences, Oslo, Norway
3. Department of Life Sciences, Roehampton University, Roehampton, UK
4. Aspetar Sports Injury and Illness Prevention Programme (ASPREV), Aspetar, Orthopeadic and Sports Medicine Hospital, Doha, Qatar
5. School of Human Movement & Nutrition Sciences, The University of Queensland, Australia

Corresponding author's contact details:

Roula Kotsifaki:

Sports City Street, P.O. Box 29222, Doha, Qatar

Argyro.Kotsifaki@aspetar.com

+ 974 50065046

ORCID: 0000-0002-7902-9206

Running title: Vertical jumps testing at RTS after ACLR and normative values

Keywords: anterior cruciate ligament, vertical jump, return to sport, performance, injury prevention

ABSTRACT

Objective Vertical jump tests are more sensitive in revealing asymmetries in performance metrics at the time of return to sport after ACL reconstruction (ACLR) than horizontal hop tests. However, it remains unclear which vertical tests (bilateral or unilateral) and which metrics (kinetics or performance) are most effective in informing the rehabilitation status and readiness for return to sport. We aimed to investigate the status of athletes during vertical jump testing at return to sport after ACLR.

Methods A dual force platform system was used to evaluate jumping performance of 126 recreational and professional athletes at the time of return to sport after ACLR, as well as 532 healthy control participants. Performance and kinetic metrics were collected during four jump tests: double leg countermovement jump, single leg countermovement jump, double leg 30-cm drop jump, and single leg 15-cm drop jump. Between-limb and between-group differences were explored using mixed models analyses.

Results At the time of return to sport after ACLR, athletes still presented significant differences favouring the uninvolved side, particularly in the symmetry of the concentric impulse ($p<0.001$) in all jumps compared to the control group. Peak landing force asymmetry was greater in the ACLR group than the controls during the countermovement ($p<0.001$, MD=-11.6; 95%CI -15.4, -7.9) and the double leg drop jump ($p=0.023$, MD=-8.9; 95%CI -14.9, -2.8). The eccentric impulse asymmetry was significantly greater ($p=0.018$, MD=-3.8; 95%CI -5.8, -1.7) in the ACLR group during the single leg drop jump only. Jump height was significantly lower ($p<0001$) in the ACLR group compared to controls in all tests except the double leg drop jump.

Conclusion At the time of return to sport after ACLR, despite passing the traditional discharge criteria, athletes remained asymmetrical during all vertical jump tests, in the concentric (push-off) phase, during landing from bilateral jumps and for most performance metrics. Clinicians should aim not only to restore ground reaction forces symmetry but also absolute performance metrics like jump height, reactive strength index, and contact times, to potentially reduce injury risk and improve overall athletic performance.

What is already known on this topic

- At the time of return to sport, athletes still present biomechanical asymmetries (joint angles, moments, and work and muscle forces) during vertical jumps, despite passing discharge criteria.
- Ground reaction force (GRF) analysis during vertical jump testing can offer valuable phase-specific information on the status of an athlete after ACLR.

What this study adds

- We report the metrics that are not yet restored at the time of return to sport, and therefore likely to be of clinical interest.
- Asymmetries were present in the concentric phase (push-off), during landing, and in most of the performance metrics.
- We provide normative data of performance metrics during vertical jumps of a large cohort of professional football players.

How this study might affect research, practice or policy

- Vertical jumps (single and bilateral) should be included in the periodic and return to sport testing after ACLR.
- Clinicians should monitor and restore symmetry and absolute performance metrics like jump height, reactive strength index, and contact times.
- Plyometric training should be an integral part of the rehabilitation protocol given the observed residual deficits seen in the single leg drop jump test.

INTRODUCTION

Functional hop testing is traditionally used to determine readiness to return to sport (RTS) after anterior cruciate ligament reconstruction (ACLR) [1] and horizontal hops are the most commonly reported tests. [2] Recent studies highlighted that horizontal hop distance is not a sensitive metric to evaluate readiness to return to sport. [3-5] Symmetry in performance on a single or triple hop for distance does not ensure symmetry in lower limb biomechanics such as joint angles, moments, and power; and muscle force contribution. [4 5] However, the hop for distance task, specifically the landing phase, can offer valuable information on the status of the knee joint—the joint-specific contributions and possible intra-limb compensations from the hip and ankle joints. [5] However, such assessments require three-dimensional biomechanical analysis, apparatus not frequently available in the clinical setting.

In contrast, vertical jump performance testing is sensitive in identifying between limb-asymmetries at the end phase of rehabilitation after ACLR[6 7] with symmetry in vertical jump height more difficult to achieve than symmetry in horizontal hop distance. [8-11] In healthy athletes vertical jump testing is a common performance assessment due to its relative simplicity and time efficiency. [12-14]

In most sports and clinical environments, the use of 3D motion capture and tri-axial force plates for biomechanical assessment is not possible due to financial and logistic constraints. However, the use of dual force platform single axis technology is increasingly common, allowing the assessment of vertical ground reaction forces and asymmetries during double and single leg jump activities. [15] Furthermore, affordable solutions such as contact measuring devices, mobile apps etc can be used to accurately assess jump performance. [16-21]

Objective testing is an integral part of the rehabilitation and the shared decision making process to allow an athlete to return to sport. [22] However, it is as yet unclear which tests and which metrics clinicians should use to track the progress of athletes during rehabilitation after ACLR, especially at the time of return to sport. There are a variety of vertical tests available (countermovement and drop jumps, double and single leg) and hundreds of metrics routinely provided by the software platforms for these tests, an overwhelming data volume for the clinician unsure which are relevant. [14]

Our hypothesis was that athletes after ACLR would still display between-limb differences as well as compared to a healthy control group during the concentric, eccentric, and landing phases during four single- and double-leg vertical tests, despite being cleared to returned to sport. Accordingly, our goal was to explore the status of the ACLR athlete for these metrics at the time of return to sport, to identify which outcomes still displayed deficits and which outcomes were sensitive to detect these using only force plates with their manufacturer-provided auto-detection software.

METHODS

We included 658 male participants, 126 eligible patients after ACLR and 532 control subjects tested in the assessment unit at Aspetar Orthopaedic and Sports Medicine Hospital, Doha, Qatar from July 2017 to July 2022. **(Table 1)**. Patients with ACLR were enrolled after the completion of a standardized rehabilitation protocol and after receiving clearance to RTS. The criteria for RTS were: 1) clearance by both their surgeon and physiotherapist, 2) completion of a sports-specific on-field rehabilitation program, 3) quadriceps strength limb symmetry index (LSI) >90%, and 4) hop battery tests with LSI >90%.[1] ACLR patients were professional or recreational athletes with a complete, unilateral ACL injury, reconstructed either with an autologous ipsilateral bone-patellar-tendon-bone (BTB) or a hamstring graft (HS) (semitendinosus and gracilis), as clinically decided by the surgeon and athlete. Participants were excluded if they had concomitant grade III knee ligament injury (other than ACL). Control subjects were male professional athletes recruited from a cohort of professional soccer players as part of an annual periodic health evaluation at the same venue. Inclusion criteria for the control group were: age range of 18 to 35 yrs, football players with no previous surgery and no history of musculoskeletal injury of the lower limb during the three months prior to testing. All participants provided informed consent, and the study was approved by the local Institutional Review Board (F2017000227 and E202009010).

Equity, diversity, and inclusion statement

Our study was on male athletes after ACLR and controls and no potential participant was excluded based on race/ethnicities, socioeconomic levels, and marginalized groups. We did not

include females due to the small number of female athletes tested (4) who met the inclusion criteria in our institution. Our author team consisted of one female (first author) and four male, junior, mid-career, and senior researchers from different disciplines, and different ethnicities.

Table 1. Participant information

	ACLR group (n=126)	Control group (n=532)
Professional athletes (n)	94	532
Age (yrs)	24 ± 6	25 ± 5
Body mass (kg)	75 ± 14	74 ± 10
Height (cm)	176 ± 9	177 ± 7
Tegner score pre-injury	8.5 ± 1.2 (range 5-10)	9.3 ± 0.4 (range 9-10)
Return to sport (months)	9.4 ± 2.6	NA
ACL graft type, n (%)		
- Hamstring	72 (57)	
- Bone-patellar-tendon-bone	54 (43)	
Isolated ACL injury	75 (60)	
Meniscal surgery	51 (40)	
- Meniscectomy	17 (13)	
- Meniscus repair	34 (27)	
Lateral augmentation	62 (49)	
- Lateral tenodesis	42 (33)	
- Antero-lateral ligament (ALL)	20 (16)	

All participants were male. Values other than number of participants are expressed as mean ± SD. ACLR, anterior cruciate ligament reconstruction.

Procedures

The complete battery of tests included, in order, the following: double countermovement jump, single leg countermovement jump, double leg drop jump from 30 cm box, and single leg drop jump from a 15 cm box. Athletes were instructed to keep their hands on their hips and jump maximally.

The jumps were examined using two ground-embedded force plates (AMTI, Watertown, MA, USA) or a dual force plate system (ForceDecks, Vald Performance, Newstead, Australia) at a sampling rate of 1000 Hz. Data were recorded with ForceDecks software (Vald Performance, Newstead, Australia) for both hardware configurations and were analysed with ForceDecks software v2.0. All participants followed a standardised warm up protocol that included 5 min

cycling on static bike and 3 double leg countermovement jumps at sub-maximum effort (perceived intensity 50%, 75% and 90%), followed by two task-specific jumps. After zeroing the plates, and weighing the athlete, each test was first demonstrated to, and then practiced by the participant. The ForceDecks software automatically identifies jump types, along with a range of metrics. The calculation methods by the software for all outcomes of interest are described in detail in the **supplementary file 1**. Events were identified by a 20 N change in ground reaction force. The jump-type identification was verified by the operator, along with jump quality, with manual removal of any mis-identified or poorly performed jumps (e.g., landing outside the force plates, arm swing, etc).

Countermovement jump

Athletes were instructed to stand fully upright, keep their hands on hips, and remain motionless for a minimum of 3 s before the initiation of the test. Athletes were asked to countermove quickly and then jump as high as possible.

Single leg countermovement jump

Athletes were instructed to stand fully upright, with 1 foot on the force plate and the free leg behind at approximately 60° knee flexion, keep their hands on hips and remain motionless for a minimum of 3 s before the initiation of the test. Athletes were asked to countermove quickly and then jump as high as possible.

Double leg drop jump

Athletes were asked to keep their hands on hips, roll from a 30-cm box with both feet together and on hitting the ground, immediately jump as high as possible while spending as little time as possible on the force plate (“as fast and as high as possible”).

Single leg drop jump

Athletes were asked to keep their hands on hips, hold their non-testing leg behind at approximately 60° knee flexion, roll from a 15-cm box and on hitting the ground, immediately jump as high as possible while spending as little time as possible on the force plate (“as fast and as high as possible”).

Test limb order was randomised for the control group. For athletes after ACLR, we first tested the uninvolved leg. Limb dominance was determined by asking the participants with which limb they would prefer to kick a ball. [23] Three trials of each test were performed with a 30 s rest period between jumps. The mean value of the 3 jumps was recorded and used for subsequent analysis. Kinetic outcomes of interest were eccentric impulse, force at zero velocity, concentric impulse, and peak landing force. For the performance metrics, variables were extracted from the best jump out of three (in terms of jump height). We used the jump height calculated by the impulse–momentum method and reactive strength index (RSI) (jump height/contact time). [24 25] LSI was determined as the percentage of the involved divided by the uninvolved leg for the ACLR group and non-dominant leg divided by dominant leg for controls for all performance and ground reaction force variables. [2 26] A symmetry of <100% indicates favouring the uninvolved leg for the ACLR group and the non-dominant for the control group.

Statistical analysis

Descriptive statistics were used to summarise the characteristics of the participants and measurements. Variables representing different aspects (concentric impulse, eccentric impulse, peak force, performance) of each phase of the jump were retained for further analyses provided they displayed sufficient precision (variance estimate compared to the group estimator). Normality of distribution of data was assessed with the Shapiro-Wilk test[27] and Q-Q plots. Between-groups (ACLR and control) comparisons were assessed using mixed effect models with subject-specific random effects. We first examined for any effect of age or activity level on symmetry (of kinetics) and found no differences, so professional and recreational athletes were explored in the same group. We then performed subgroup analyses to evaluate the effect of graft on kinetic symmetry and performance outcomes using one-way ANOVA with post hoc comparisons adjusted for multiple comparisons (Tukey). For the performance metrics, however, there were significant differences between professional and recreational athletes. Accordingly for the analyses of performance, comparisons were performed only between professional athletes after ACLR and a control group of professional athletes. For the performance metrics during single leg jumps in the control group, exploratory analyses examined for differences between dominant/non-dominant legs. As there were no significant differences for these metrics,

a randomly chosen leg was used for subsequent analyses. Post hoc comparisons (Tukey) were performed to adjust for multiple comparisons where applicable (single leg jumps comparing the involved leg, the uninvolved leg, and the controls). A $p<0.05$ was considered statistically significant. Effect sizes (ES) were calculated using the pooled weighted standard deviation. [28] Analyses were performed using SPSS v.26 (IBM Corporation, Armonk, NY) and the mixed models using JMP V.16 (SAS Institute).

RESULTS

Participants were tested within 2 weeks of clearance to RTS. Subgroup comparisons of graft types showed some differences for kinetics symmetry (**supplementary file 2).** There was an effect of activity level on performance metrics; hence all comparisons on performance outcomes were performed only between professional athletes after ACLR and a control group of professional athletes **(supplementary file 3).** We did not include recreational athletes in the comparisons of performance metrics however, we report their descriptive outcomes for reference. All metrics that were examined are presented in **supplementary file 4**.

Countermovement jump

There was no difference between athletes after ACLR and the control group for the symmetry during the eccentric phase, or at the transition between eccentric and concentric (force at zero velocity). Conversely, there were significant differences during the concentric phase, especially in the second half (concentric impulse P2). Peak landing force symmetry was significantly different between groups. Jump height in the professional athletes after ACLR did not reach the values of the control group **(Figure 1, Table 2, and supplementary file 3).**

Single leg countermovement jump

There was no difference between groups for the eccentric deceleration impulse symmetry and no difference for the force at zero velocity symmetry. Similar to the countermovement jump, significant differences were found for the concentric impulse symmetry. There was no difference in peak landing force symmetry. Jump height in the professional athletes after ACLR was

significantly less than their uninvolved limb and did not reach the jump height of the control group **(Figure 1, Table 2, and supplementary file 3).**

Double leg drop jump

There was no difference between ACLR and healthy groups in the eccentric impulse symmetry. There was a difference for the force at zero velocity symmetry between groups. Significant differences were observed for the concentric and landing impulses symmetry. In terms of performance, significant differences were found for contact time and RSI but not for jump height between professional athletes after ACLR and the control group **(Figure 1, Table 2, and supplementary file 3).**

Single leg drop jump

There were significant differences in the eccentric impulse, force at zero velocity, and the concentric impulse symmetries between athletes after ACLR and the control group. There was no difference in symmetry of peak force during landing. In terms of performance, there were still significant differences between legs in athletes after ACLR for jump height and RSI. Importantly, neither involved nor uninvolved limbs reached the performance values of the control group in any of the performance metrics **(Figure 1, Table 2, and supplementary file 3).**

Subgroup analysis by graft

Subgroup analysis revealed differences between graft types for the concentric impulse symmetry during the countermovement jump and for force symmetry at zero velocity during the countermovement jumps (single and double) and the single leg drop jump. Athletes with BTB graft were more asymmetrical than athletes with HS graft. There were no differences between groups for the performance metrics based on graft type (**Supplementary file 2).**

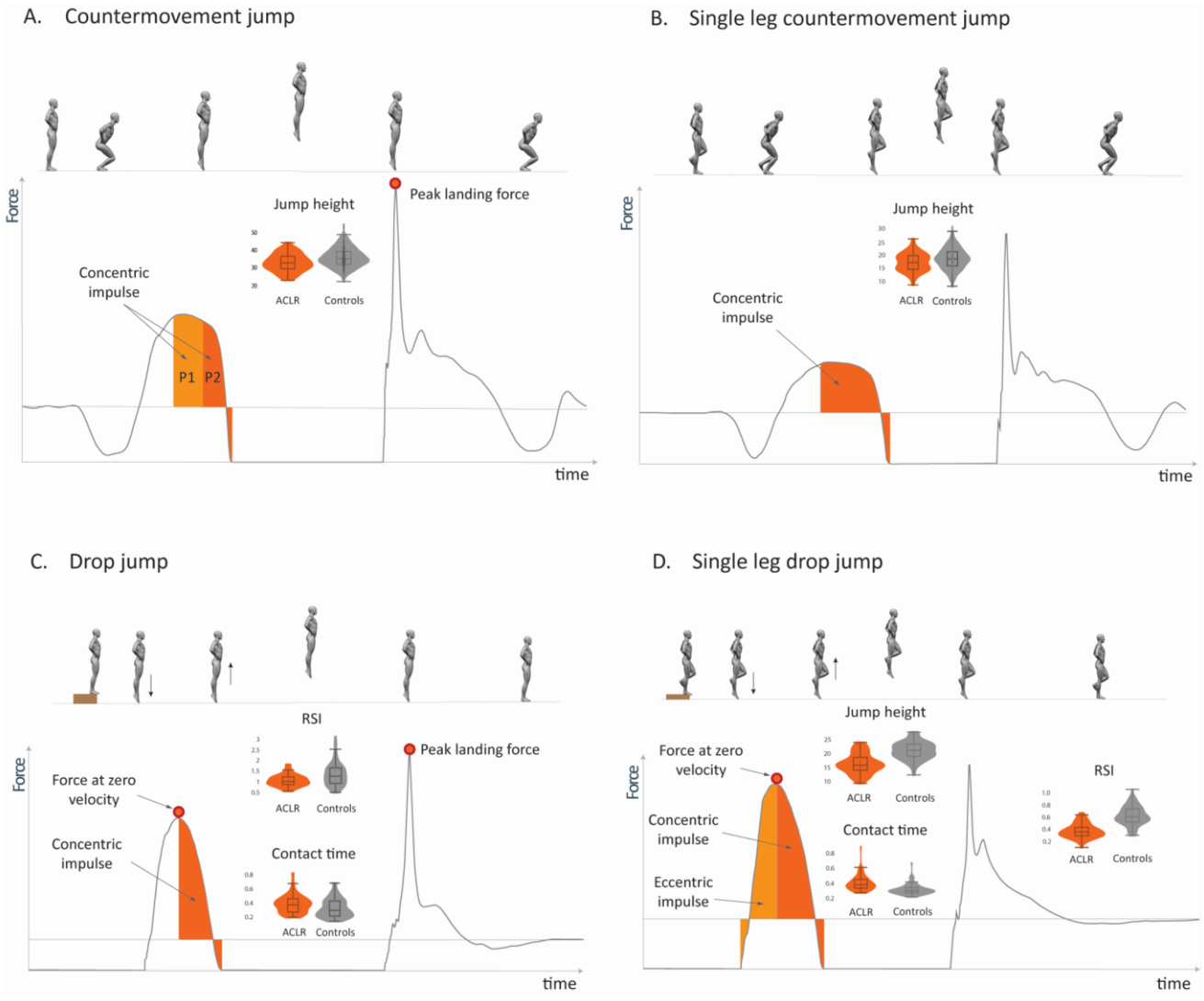

Figure 1. Examples of force-time curves for: A. Countermovement jump, B. Single leg countermovement jump, C. Drop jump, D. Single leg drop jump, with the metrics with significant differences between athletes after ACLR and controls. **Concentric impulse (N/s):** area under the vertical force curve from transition point at zero velocity (max negative displacement) (start of concentric phase) to take-off - net impulse. **Concentric impulse P2 (N/s):** Net impulse during 2nd 50% (timewise) of concentric phase. **Jump height (cm):** Jump height calculated by the impulse–momentum method. **Peak landing force (N):** Peak force as the athlete lands following the jump. **Force at zero velocity (N):** The force at the instant velocity is zero prior to takeoff. **Reactive strength index (RSI):** Jump height divided by contact time.

Table 2. Comparison of kinetic symmetries between groups during vertical jumps

Countermovement jump	**ACLR** n=126		**Controls** n=532				
	Mean ± SD	CV%	Mean ± SD	CV%	p value	d	Mean difference (95% CIs)
Eccentric deceleration impulse	96 ± 13	13	97 ± 14	15	0.41		-0.9 (-3.7, 1.8)
Force at zero velocity	96 ± 11	12	97 ± 12	12	0.09		-1.7 (-4.0, 0.6)
Concentric impulse_P1	95 ± 8	9	98 ± 8	8	**<0.001**	-0.42 (-0.61, -0.22)	-3.5 (-5.1, -1.9)
Concentric impulse_P2	90 ± 8	9	100 ± 7	7	**<0.001**	-1.42 (-1.63, -1.21)	-10.3 (-11.7, -8.9)
Concentric impulse	93 ± 7	8	99 ± 7	7	**<0.001**	-0.95 (-1.15, -0.75)	-6.5 (-7.9, -5.2)
Peak landing force	90 ± 20	22	101 ± 19	19	**<0.001**	-0.60 (-0.80, -0.41)	-11.6 (-15.4, -7.9)
Single leg jump	**ACLR** n=118		**Controls** n=516		p value	d	Mean difference (95% CIs)
Eccentric deceleration impulse	94 ± 18	19	99 ± 28	28	0.12		-5.0 (-9.0, 0.3)
Force at zero velocity	98 ± 9	10	99 ± 10	10	0.19		-1.4 (-3.4, 0.6)
Concentric impulse	92 ± 6	7	101 ± 8	8	**<0.001**	-1.11 (-1.32, -0.90)	-8.5 (-10.0, -7.0)
Peak landing force	99 ± 12	12	100 ± 13	13	0.91		-0.5 (-3.0, 2.0)
Drop jump	**ACLR** n=65		**Controls** n=100		p value	d	Mean difference (95% CIs)
Eccentric impulse	92 ± 14	15	98 ± 24	25	0.23		-5.2 (-11.7, 1.2)
Force at zero velocity	92 ± 11	12	97 ± 13	14	**0.036**	-0.35 (-0.67, -0.04)	-4.5 (-8.3, -0.6)
Concentric impulse	89 ± 11	12	100 ± 11	11	**<0.001**	-0.96 (-1.29, -0.63)	-10.5 (-14.0, -7.1)
Peak landing force	93 ± 17	19	101 ± 20	20	**0.023**	-0.46 (-0.78, -0.15)	-8.9 (-14.9, -2.8)
Single leg drop jump	**ACLR** n=110		**Controls** n=123		p value	d	Mean difference (95% CIs)
Eccentric impulse	96 ± 7	7	99 ± 8	8	**0.018**	-0.48 (-0.74, -0.22)	-3.8 (-5.8, -1.7)
Force at zero velocity	92 ± 11	12	101 ± 11	11	**<0.001**	-0.84 (-1.11, -0.57)	-9.2 (-12.1, -6.4)
Concentric impulse	92 ± 6	7	101 ± 6	6	**<0.001**	-1.35 (-1.67, -1.05)	-8.8 (-10.4, -7.1)
Peak landing force	98 ± 11	11	99 ± 14	14	0.96		-1.4 (-4.7, 1.8)

ACLR, anterior cruciate ligament reconstruction; symmetries are presented as percentages ± standard deviation (involved limb / uninvolved limb) for the ACLR cohort, and (non-dominant limb/dominant limb) for the control cohort; d: Cohen's d (effect size).

Performance metrics by activity level and normative values

Performance metrics for the ACLR population (professional and recreational athletes) at the time of return to sport, and normative data from professional football players are summarised in **table 3**.

Table 3. Performance metrics by activity level in athletes after ACLR and healthy professional athletes.

Countermovement jump	Recreational athletes - ACLR	Professional athletes - ACLR	Professional athletes		
Jump height	28.3 ± 6.0	33.3 ± 5.0	36.3 ± 5.4		
Drop jump	Recreational athletes - ACLR	Professional athletes - ACLR	Professional athletes		
Jump height	27.3 ± 56.7	35.9 ± 5.9	36.1 ± 5.2		
Contact time	0.37 ± 0.09	0.39 ± 0.12	0.34 ± 0.13		
RSI	0.9 ± 0.3	1.09 ± 0.3	1.38 ± 0.5		
Single leg jump	Recreational athletes - INV	Recreational athletes - UNINV	Professional athletes - INV	Professional athletes - UNINV	Professional athletes - Controls
Jump height	10.5 ± 3.6	12.7 ± 3.4	14.2 ± 3.4	16.5 ± 3.3	17.4 ± 3.7
Single leg drop jump	Recreational athletes - INV	Recreational athletes - UNINV	Professional athletes - INV	Professional athletes - UNINV	Professional athletes - Controls
Jump height	11.3 ± 3.9	13.7 ± 4.1	14.6 ± 3.5	17.1 ± 3.6	18.5 ± 2.9
Contact time	0.41 ± 0.06	0.38 ± 0.05	0.41 ± 0.10	0.38 ± 0.09	0.33 ± 0.07
RSI	0.29 ± 0.12	0.37 ± 0.14	0.38 ± 0.12	0.47 ± 0.14	0.58 ± 0.13

RSI, reactive strength index; INV, involved leg; UNINV, uninvolved leg.

DISCUSSION

We have identified the vertical jump characteristics which are not yet restored at the time of RTS after ACLR, and we provide normative performance data for professional football players. The most significant residual deficits were in the concentric phase, and in the performance metrics across all jumps investigated. The single leg drop jump was the most sensitive test to reveal asymmetries in kinetics and performance metrics and the countermovement jump to expose landing asymmetries. The deficits we identify in this large cohort confirm our previous findings: 1) that ACLR patients show significant kinetic deficits despite meeting RTS criteria and 2) that vertical jump tests are sensitive to uncover those deficits. Kinetics asymmetries were most prominent during the concentric phase across all jumps examined. We found no differences in the eccentric deceleration impulse at the time of return to sport. The asymmetries still present during the concentric phase are in agreement with previous research in professional football players at 9 months after surgery[29] and previous studies in elite skiers at 2 years after surgery.[30]

Concentric phase asymmetries

During the countermovement jump the difference in concentric phase symmetry between groups was more prominent during the second 50% (timewise) of the concentric phase. A possible explanation might be the role of ankle plantar flexors. Our recent research on a similar population showed that soleus muscle contribution was significantly less in both legs of athletes after ACLR compared to a control group during the concentric phase of a horizontal and a vertical jump. [5 7] Previous research suggests that medial gastrocnemius onset occurs later in a countermovement jump than other muscles and that peak activation occurs at approximately 83% into the jump, which reinforces the suggestion that plantar flexors play an important role in force generation during the late jump phase. [31]

Additionally, a recent study reported a lack of recovery of body velocity in the final phase of take-off and suggested the sustained impairments in plantar flexor muscle function in both the affected and non-affected limbs as a possible reason. [32] Finally, during a single leg squat jump, a 34% decrease in maximal ankle power between limbs in patients after ACLR was reported, not from an alteration in joint moment but from a decrease in the angular velocity of ankle plantar flexion. [33]

Performance metrics asymmetries

Performance metrics were still not restored in all types of jumps examined. In unilateral jumps, there are differences between limbs, while in bilateral jumps, there are differences between the ACLR and control groups. Jump performance (jump height) is a critical performance metric that is closely related to the concentric phase of a vertical jump task. The ability to take off with powerful extension of the hip, knee, and ankle is essential for achieving maximum jump height. [25] Control participants displayed symmetry in jump height, which suggests that symmetrical measures will be critical for assessing rehabilitation completion and should be used as a criterion to ensure that athletes are back to their pre-injury levels. It seems that the task of restoring vertical jump symmetry is more challenging than restoring symmetry in strength or hop distance especially since our athletes have exceed the 90% threshold and were cleared to return to sport. Fortunately, for clinicians, kinetic asymmetries are also evident in performance asymmetries, which can be easily detected without the need of advanced equipment. Recent improvements

in technology allow the use for valid and reliable alternative methods to measure vertical jump performance, such as low-cost force plates, contact mats, photoelectric cells or even mobile applications. [16-21]

The literature is scarce on performance metrics during vertical jumps in athletes after ACLR. Jump height increases linearly with greater time post-surgery during a countermovement jump; [29] however, at 6 months[34] and 9 months[29] after surgery the jump height remains significantly lower than that of healthy matched controls.

The single leg drop jump test

The single leg drop jump showed significant differences between groups in all phases (except landing) and performance outcomes. At the time of return to sport after ACLR, athletes still did not reach symmetry in kinetics and performance metrics, favouring the uninvolved side. Single leg drop jumps appear to better expose knee deficits in those recovering from ACL injury. Briefly, the individual components of the single leg drop jump - eccentric and concentric force - shed light on the leg's load acceptance and generating capacity, respectively. Also, highlighted the large differences in performance metrics like jump height and contact time. Deficits identified in comparison to the uninjured limb and compared to normative data for similar athletes can then be targeted through tailored rehabilitation. Reactive tests (drop jumps) are important to evaluate other performance parameters like power and reactivity. Plyometric training may improve subjective function and functional activities compared to usual rehabilitation care, without any increase in laxity or pain and should be an integral part of the rehabilitation protocol. [35] Most research on reactive jumps emphasize double-leg drop jumps[36-38] and there is not much research on single leg drop jump metrics after ACLR. [39] Our recent study reported a 70% difference in knee work between limbs in the concentric phase in athletes at the time of return to sport. [7] Residual deficits during single leg drop jump were evident also in the performance metrics with an asymmetry in 20-30% for jump height and RSI at 9 months after surgery. [7 9]

Bilateral or unilateral test?

Bilateral and unilateral tests are both important and provide different information for the athlete's status. Bilateral tests are useful to evaluate a patient's inter-limb compensatory movement

strategies and unilateral tests offer an opportunity to assess a single limb's performance capacity in isolation which can additionally be compared to the contralateral limb as well as normative reference data. In the current study, we found differences in both double leg tasks (countermovement and drop jump) during landing, indicating that athletes still shift their weight during landing to the uninvolved leg. In our exploratory analysis during the countermovement jump we evaluated results for both peak landing force and landing impulse. The landing impulse metric had greater variance (trial-to-trial differences) in both athletes after ACLR and controls, so we suggest using the peak landing force metric instead of landing impulse. Unilateral tests are useful to evaluate the ability of each limb to perform independently. In patients after ACLR it is common to compensate for lower knee work with greater hip and ankle work[5 7] however, these intra-limb compensations cannot be detected by the uniaxial force plates and require three-dimensional biomechanical analysis, apparatus not frequently available in the clinical setting. In the absence of advanced equipment, clinicians can use performance metrics-like jump height-during unilateral vertical tests to evaluate the overall lower limb functional status of the athletes. Peak landing force in unilateral tests did not reveal any statistically or clinically important differences and is not recommended as a useful metric.

Influence of graft choice

Graft choice had an influence on kinetic asymmetries in specific outcomes, with BTB procedures resulting in greater asymmetry. The transition between eccentric and concentric phase (force at zero velocity) was the metric influenced mostly by the graft type and there were greater asymmetries in all tests with a BTB graft. Previous research reports that during a countermovement jump at 9 months after ACLR, athletes with a BTB graft had greater inter-limb impulse asymmetries than athletes with a HS graft in the eccentric deceleration and concentric phases of the countermovement jump, although similar jump heights were achieved. [40] During landing there was a significant difference between ACLR and control groups, but no difference between BTB and HS graft, in agreement with previous research. [40]

Is symmetry important?

The goal of rehabilitation is to return the athlete back to normal. It is difficult to define normal, as this is different for each patient. Clinicians should use asymmetry metrics on an individual level

and by comparing to the noise of each test and each metric. [41] Normally, the clinician does not have preoperative test values to set the end goals for each patient. [42] Achieving symmetry is an important goal during rehabilitation, but equally important is to return the athlete to their previous level of performance. We suggest that the uninvolved limb should be monitored during rehabilitation, and both limbs should reach matched-control normative values in the absence of pre-operative data. In our healthy cohort we report the performance outcomes for each of the tests. These can be used by the clinicians to set a target for their patients where pre-operative values are not available. Although symmetry and its importance has been questioned, we cannot deny the fact that, consistent with previous findings, [30 32] the between-limb asymmetry in the control group was small in all the variables explored, except landing. The standard deviation of each variable is also reported to help the clinician interpret any differences. There was no statistically significant difference between limbs in the control group for performance metrics during the single leg jumps. Limb dominance did not affect the performance of these tests in football players; this might not apply in other sports.

Clinical implications

We present between-leg asymmetries during four vertical jump tests in athletes after ACLR who were cleared to RTS and compare them with a large healthy cohort. Clinicians can use these results to inform their clinical practice and restore the phase-specific asymmetries. We emphasize the importance of restoring symmetry between legs – not only in jump testing – in patients who undergo a long rehabilitation period; however, this is not enough. Absolute performance metrics are not fully restored for the involved and the uninvolved leg and clinicians should target also restoring vertical jump capacity in both legs. Our study provides performance metrics for the ACLR population (professional and recreational athletes) at the time of return to sport, and normative data from professional football players which can be used as a target by clinicians working with similar populations.

The residual deficits seen in single leg drop jump suggest that athletes were not exposed enough plyometric training. Plyometric drills are fundamental components of most sports and an important neuromuscular quality closely associated with performance in explosive sports. [43] Additionally, rehabilitation should target not only strength restoration of the quadriceps and

hamstrings, but also the ankle plantar flexors as they might be important component of vertical jump capacity.

Bilateral jumps best described landing asymmetries, but clinicians should be mindful of the relatively high population variance, even in the control group, when interpreting the results.

Limitations and future directions

We included only males from a single institution and the generalizability of these results to other populations is unknown. Particularly the performance normative metrics and the asymmetry results (with their corresponding variance) can vary widely based on sport, activity level, and gender which limits comparisons between groups. In the current study normative data are for professional football players and the results presented might be different in other sports. We did not include normative data for recreational athletes to evaluate if our patients restored performance metrics or not. Future studies should report vertical jump performance metrics for female and recreational athletes of different sports. We investigated outcomes at a single time point, at the time of return to sport. During rehabilitation there might be additional important metrics to track an athlete's progression, that normalize before the time of return to sport. We need longitudinal studies during the rehabilitation period to describe these metrics. Correct execution of the tests is an important parameter that can affect the results. Although we instructed athletes to countermove fast, we didn't control the peak eccentric velocity, that is we didn't set a threshold on that metric to increase consistency. However, exploring the results there was no difference in peak eccentric velocity between groups.

All metrics that were examined have been presented, yet these objectively large number of measures remain a subset of all possible jump metrics. Future research should consider pre-registration of outcomes to reduce the possibility of false positive results. More studies are needed to evaluate the differences found mostly in the concentric phase and if this finding is related to the rehabilitation approach or it is a common finding seen in athletes after ACLR. Further research is required to determine the value of vertical jump testing at the time of return to sport and the relationship between the residual functional asymmetries and the risk of future injury (e.g., graft tear or contralateral ACL injury, meniscal and chondral injuries, osteoarthritis).

CONCLUSION

Vertical jumps testing offers valuable phase-specific information on the status of the athlete after ACLR and should be included in the periodic and RTS assessment. In our cohort there were still asymmetries in the concentric (push-off) phase, during landing of bilateral jumps, and most of the performance metrics, despite passing the traditional discharge criteria. Apart from symmetry clinicians should target restoring absolute performance metrics like jump height, reactive strength index, and contact times.

Twitter Roula Kotsifaki @RoulaKotsifaki, Rodney Whiteley @RodWhiteley, Enda King @enda_king, Roald Bahr @RoaldBahr, Vasileios Sideris @vasilisbme.

Acknowledgements The authors thank the physiotherapists (ACL Group) of Aspetar Rehabilitation Department for assisting with subjects' recruitment.

Contributors RK and RW participated in the conception and the design of the study. RK and VS were responsible for data collection. RK performed the data analysis and table designs and all the authors contributed to the interpretation. RK drafted the manuscript, and all the authors revised it critically and gave their approval of the final version.

Funding The authors have not declared a specific grant for this research from any funding agency in the public, commercial or not-for-profit sectors.

Competing interests None declared.

Patients involvement Patients or the public were not involved in the design, or conduct, or reporting, or dissemination plans of our research.

Patient consent for publication Not required.

Ethics approval Ethics approval was granted from the local Institutional Review Board (F2017000227 and E202009010).

Provenance and peer review Not commissioned, externally peer reviewed.

Data availability statement Data are available upon reasonable request.

ORCID iD

Roula Kotsifaki 0000-0002-7902-9206

Enda King 0000-0003-0434-1489

Roald Bahr 0000-0001-5725-4237

Rodney Whiteley 0000-0002-1452-6228

REFERENCES

1. Kyritsis P, Bahr R, Landreau P, et al. Likelihood of ACL graft rupture: not meeting six clinical discharge criteria before return to sport is associated with a four times greater risk of rupture. *Br J Sports Med* 2016;50(15):946-51.
2. Abrams GD, Harris JD, Gupta AK, et al. Functional Performance Testing After Anterior Cruciate Ligament Reconstruction: A Systematic Review. *Orthop J Sports Med* 2014;2(1):2325967113518305.
3. Kotsifaki A, Korakakis V, Whiteley R, et al. Measuring only hop distance during single leg hop testing is insufficient to detect deficits in knee function after ACL reconstruction: a systematic review and meta-analysis. *Br J Sports Med* 2020;54(3):139-53.
4. Kotsifaki A, Van Rossom S, Whiteley R, et al. Symmetry in Triple Hop Distance Hides Asymmetries in Knee Function After ACL Reconstruction in Athletes at Return to Sports. *Am J Sports Med* 2022;50(2):441-50.
5. Kotsifaki A, Whiteley R, Van Rossom S, et al. Single leg hop for distance symmetry masks lower limb biomechanics: time to discuss hop distance as decision criterion for return to sport after ACL reconstruction? *Br J Sports Med* 2022;56(5):249-56.
6. Kotsifaki A, Korakakis V, Graham-Smith P, et al. Vertical and Horizontal Hop Performance: Contributions of the Hip, Knee, and Ankle. *Sports Health* 2021;13(2):128-35.
7. Kotsifaki A, Van Rossom S, Whiteley R, et al. Single leg vertical jump performance identifies knee function deficits at return to sport after ACL reconstruction in male athletes. *Br J Sports Med* 2022;56(9):490-98.
8. Ebert JR, Du Preez L, Furzer B, et al. Which Hop Tests Can Best Identify Functional Limb Asymmetry in Patients 9-12 Months After Anterior Cruciate Ligament Reconstruction Employing a Hamstrings Tendon Autograft? *Int J Sports Phys Ther* 2021;16(2):393-403.
9. King E, Richter C, Franklyn-Miller A, et al. Whole-body biomechanical differences between limbs exist 9 months after ACL reconstruction across jump/landing tasks. *Scand J Med Sci Sports* 2018;28(12):2567-78.
10. King E, Richter C, Franklyn-Miller A, et al. Back to normal symmetry? Biomechanical variables remain more asymmetrical than normal during jump and change-of-direction

testing 9 months after anterior cruciate ligament reconstruction. *Am J Sports Med* 2019;47(5):1175-85.

11. Ohji S, Aizawa J, Hirohata K, et al. Single-leg hop can result in higher limb symmetry index than isokinetic strength and single-leg vertical jump following anterior cruciate ligament reconstruction. *Knee* 2021;29:160-66.
12. Bishop C, Jordan M, Torres-Ronda L, et al. Selecting Metrics That Matter: Comparing the Use of the Countermovement Jump for Performance Profiling, Neuromuscular Fatigue Monitoring, and Injury Rehabilitation Testing. *Strength Cond J* 2022:10.1519.
13. Bishop C, Turner A, Jarvis P, et al. Considerations for Selecting Field-Based Strength and Power Fitness Tests to Measure Asymmetries. *J Strength Cond Res* 2017;31(9):2635-44.
14. Bishop C, Turner A, Jordan M, et al. A Framework to Guide Practitioners for Selecting Metrics During the Countermovement and Drop Jump Tests. *Strength Cond J* 2022;44(4):95-103.
15. Cohen D, Burton A, Wells C, et al. Single vs Double Leg Countermovement Jump Tests: Not half an Apple! *Aspetar Sport Med J* 2020;9:34-41.
16. Brooks ER, Benson AC, Bruce LM. Novel Technologies Found to be Valid and Reliable for the Measurement of Vertical Jump Height With Jump-and-Reach Testing. *J Strength Cond Res* 2018;32(10):2838-45.
17. Haynes T, Bishop C, Antrobus M, et al. The validity and reliability of the My Jump 2 app for measuring the reactive strength index and drop jump performance. *J Sports Med Phys Fitness* 2019;59(2):253-58.
18. Healy R, Kenny IC, Harrison AJ. Assessing Reactive Strength Measures in Jumping and Hopping Using the Optojump™ System. *J Hum Kinet* 2016;54:23-32.
19. Pueo B, Lipinska P, Jiménez-Olmedo JM, et al. Accuracy of Jump-Mat Systems for Measuring Jump Height. *Int J Sports Physiol Perform* 2017;12(7):959-63.
20. Balsalobre-Fernández C, Glaister M, Lockey RA. The validity and reliability of an iPhone app for measuring vertical jump performance. *J Sports Sci* 2015;33(15):1574-9.
21. Stanton R, Kean CO, Scanlan AT. My Jump for vertical jump assessment. *Br J Sports Med* 2015;49(17):1157-58.

22. Ardern CL, Glasgow P, Schneiders A, et al. 2016 Consensus statement on return to sport from the First World Congress in Sports Physical Therapy, Bern. *Br J Sports Med* 2016;50(14):853-64.
23. van Melick N, Meddeler BM, Hoogeboom TJ, et al. How to determine leg dominance: The agreement between self-reported and observed performance in healthy adults. *PloS One* 2017;12(12):e0189876.
24. Healy R, Kenny IC, Harrison AJ. Reactive Strength Index: A Poor Indicator of Reactive Strength? *Int J Sports Physiol Perform* 2018;13(6):802-09.
25. Linthorne NP. Analysis of standing vertical jumps using a force platform. *Am J Phys* 2001;69(11):1198-204.
26. Noyes FR, Barber SD, Mangine RE. Abnormal lower limb symmetry determined by function hop tests after anterior cruciate ligament rupture. *Am J Sports Med* 1991;19(5):513-8.
27. Shapiro SS, Wilk MB. An analysis of variance test for normality (complete samples). *Biometrika* 1965;52(3/4):591-611.
28. Hedges L, Olkin I. Statistical methods for meta-analysis: Academic press 2014.
29. Read PJ, Michael Auliffe S, Wilson MG, et al. Lower Limb Kinetic Asymmetries in Professional Soccer Players With and Without Anterior Cruciate Ligament Reconstruction: Nine Months Is Not Enough Time to Restore "Functional" Symmetry or Return to Performance. *Am J Sports Med* 2020;48(6):1365-73.
30. Jordan MJ, Aagaard P, Herzog W. Lower limb asymmetry in mechanical muscle function: A comparison between ski racers with and without ACL reconstruction. *Scand J Med Sci Sports* 2015;25(3):e301-9.
31. Sahrom SB, Wilkie JC, Nosaka K, et al. The use of yank-time signal as an alternative to identify kinematic events and define phases in human countermovement jumping. *R Soc Open Sci* 2020;7(8):192093.
32. Jordan MJ, Morris N, Nimphius S, et al. Attenuated Lower Limb Stretch-Shorten-Cycle Capacity in ACL Injured vs. Non-Injured Female Alpine Ski Racers: Not Just a Matter of Between-Limb Asymmetry. *Front Sports Act Living* 2022;4:853701.

33. de Fontenay BP, Argaud S, Blache Y, et al. Motion alterations after anterior cruciate ligament reconstruction: comparison of the injured and uninjured lower limbs during a single-legged jump. *J Athl Train* 2014;49(3):311-6.
34. O'Malley E, Richter C, King E, et al. Countermovement Jump and Isokinetic Dynamometry as Measures of Rehabilitation Status After Anterior Cruciate Ligament Reconstruction. *J Athl Train* 2018;53(7):687-95.
35. Kotsifaki R, Korakakis V, King E, et al. Aspetar clinical practice guideline on rehabilitation after anterior cruciate ligament reconstruction. *Br J Sports Med* 2023;**57:**500-514.
36. Myer GD, Ford KR, Khoury J, et al. Development and validation of a clinic-based prediction tool to identify female athletes at high risk for anterior cruciate ligament injury. *Am J Sports Med* 2010;38(10):2025-33.
37. Nilstad A, Andersen TE, Kristianslund E, et al. Physiotherapists can identify female football players with high knee valgus angles during vertical drop jumps using real-time observational screening. *J Orthop Sports Phys Ther* 2014;44(5):358-65.
38. Noyes FR, Barber-Westin SD, Fleckenstein C, et al. The drop-jump screening test: difference in lower limb control by gender and effect of neuromuscular training in female athletes. *Am J Sports Med* 2005;33(2):197-207.
39. Maestroni L, Read P, Turner A, et al. Strength, rate of force development, power and reactive strength in adult male athletic populations post anterior cruciate ligament reconstruction - A systematic review and meta-analysis. *Phys Ther Sport* 2021;47:91-104.
40. Miles JJ, King E, Falvey É C, et al. Patellar and hamstring autografts are associated with different jump task loading asymmetries after ACL reconstruction. *Scand J Med Sci Sports* 2019;29(8):1212-22.
41. Bishop C, Lake J, Loturco I, et al. Interlimb Asymmetries: The Need for an Individual Approach to Data Analysis. *J Strength Cond Res* 2021;35(3):695-701.
42. Wellsandt E, Failla MJ, Snyder-Mackler L. Limb symmetry indexes can overestimate knee function after anterior cruciate ligament injury. *J Orthop Sports Phys Ther* 2017;47(5):334-38.
43. Booth MA, Orr R. Effects of plyometric training on sports performance. *Strength Cond J* 2016;38(1):30-37.

Supplementary file 1

Eccentric deceleration impulse

Area under the force curve during the eccentric phase (contact to the transition point at zero velocity (max negative displacement)).

Force at zero velocity

The combined (total) force at the instant velocity is zero prior to take-off.

Concentric impulse

Area under the force curve during the concentric phase (from transition point at zero velocity (max negative displacement) to take-off).

Concentric impulse_P2

Concentric impulse during 2nd 50% (timewise) of concentric phase.

Peak landing force

Peak force as the athlete lands following the jump.

Jump height

Maximum jump height calculated using the impulse-momentum theorem (utilizing takeoff velocity).

Contact time

Contact time is the time spent on the ground (during the reactive phase).

RSI

Reactive Strength Index (RSI) = Jump height / Contact time.

Supplementary file 2

Table. Comparison of kinetic symmetries between groups by graft type

	BTB	HS	Controls	BTB - HS			BTB - CONTROLS			HS - CONTROLS		
Countermovement jump	**BTB n=54**	**HS n=72**	**Controls n=532**	**p value**	**d**	**Mean difference (95% CIs)**	**p value**	**d**	**Mean difference (95% CIs)**	**p value**	**d**	**Mean difference (95% CIs)**
Eccentric deceleration impulse	93±13	98±13	97±14	0.15		-4.7 (-10.7, 1.2)	0.17		-3.6 (-8.3, 1.1)	0.80		1.1 (-3.0, 5.3)
Force at zero velocity	92±11	98±11	97±12	**0.015**	0.53	-5.8 (-10.8, -0.9)	**0.007**	0.43	-5.1 (-9.0, -1.2)	0.86		0.8 (-2.7, 4.2)
Concentric impulse_P1	92±8	97±8	98±8	**0.001**	0.67	-5.4 (-8.9, -1.9)	**<0.001**	0.81	-6.6 (-9.3, -3.8)	0.50		-1.2 (-3.6, 1.3)
Concentric impulse_P2	88±7	91±9	100±7	**0.042**	0.40	-3.1 (-6.2, -0.1)	**<0.001**	1.73	-12.1 (-14.5, -9.7)	**<0.001**	1.23	-9.0 (-11.1, -6.8)
Concentric impulse	90±6	94±8	99±7	**0.001**	0.62	-4.4 (-7.3, -1.5)	**<0.001**	1.33	-9.0 (-11.3, -6.8)	**<0.001**	0.67	-4.7 (-6.7, -2.6)
Peak landing force	85±18	93±21	101±19	**0.05**		-8.1 (-16.2, 0.1)	**<0.001**	0.85	-16.2 (-22.7, -9.8)	**0.002**	0.42	-8.1 (-13.8, -2.5)
	BTB n=48	**HS n=46**	**Controls n=532**									
Jump height	33.7±5.0	32.9±5.1	36.3±5.4	0.76		0.8 (-1.8, 3.4)	**0.005**	0.48	-2.6 (-4.5, -0.7)	**<0.001**	0.63	-3.4 (-5.3, -1.4)
Single leg jump	**BTB n=51**	**HS n=67**	**Controls n=516**	**p value**	**d**	**Mean difference (95% CIs)**	**p value**	**d**	**Mean difference (95% CIs)**	**p value**	**d**	**Mean difference (95% CIs)**
Eccentric deceleration impulse	91±17	97±18	99±28	0.46		-5.9 (-17.4, 5.6)	0.08		-8.3 (-17.4, 0.7)	0.74		-2.5 (-10.5, 5.6)
Force at zero velocity	95±9	100±9	99±10	**0.008**	0.62	-5.6 (-10.0, -1.3)	**0.005**	0.45	-4.6 (-8.1, -1.2)	0.73		1.02 (-2.0, 4.1)
Concentric impulse	92±6	93±6	100±8	0.6		-1.2 (-4.5, 2.2)	**<0.001**	1.11	-9.2 (-11.8, -6.5)	**<0.001**	0.97	-8.0 (-10.3, -5.7)
Peak landing force	100±13	98±12	100±13	0.77		1.6 (-3.9, 7.2)	0.98		0.4 (-4.0, 4.8)	0.73		-1.2 (-5.1, 2.6)
	BTB n=45	**HS n=41**	**Controls n=516**									
Jump height symmetry	84±10	89±13	102±18	0.37		-5.0 (-13.9, 3.8)	**<0.001**	0.99	-17.7 (-24.0, -11.3)	**<0.001**	0.71	-12.7 (-19.3, -6.0)
Drop jump	**BTB n=22**	**HS n=43**	**Controls n=100**	**p value**	**d**	**Mean difference (95% CIs)**	**p value**	**d**	**Mean difference (95% CIs)**	**p value**	**d**	**Mean difference (95% CIs)**
Eccentric impulse	88±15	95±13	98±24	0.45		-6.5 (-19.2, 6.2)	0.12		-9.5 (-21.0, 1.9)	0.70		-3.1 (-11.9, 5.8)
Force at zero velocity	89±12	94±11	97±13	0.26		-5.1 (-12.9, 2.6)	0.022	0.60	-7.9 (-14.8, -0.9)	0.46		-2.7 (-8.1, 2.7)
Concentric impulse	87±11	90±11	100±11	0.41		-3.6 (-10.4, 3.1)	**<0.001**	1.18	-12.9 (-19.0, -6.9)	**<0.001**	0.86	-9.3 (-14.0, -4.6)
Peak landing force	94±20	92±16	101±20	0.95		1.6 (-10.4, 13.5)	0.20		-7.9 (-18.6, 2.9)	**0.022**	0.49	-9.4 (-17.7, -1.1)
	BTB n=19	**HS n=24**	**Controls n=100**									
Jump height	36.4±5.7	35.5±6.2	36.1±5.2	0.82		1.0 (-2.9, 4.8)	0.96		0.4 (-2.7, 3.5)	0.88		-0.6 (-3.4, 2.2)
Contact time	0.42±0.11	0.37±0.13	0.34±0.13	0.34		0.05 (-0.04, 0.15)	**0.023**	0.63	0.08 (0.01, 0.16)	0.56		0.03 (-0.04, 0.1)
RSI	1.03±0.29	1.12±0.29	1.38±0.55	0.81		-0.09 (-0.44, 0.26)	0.015	0.67	-0.34 (-0.63, -0.06)	0.06		-0.25 (-0.51, 0.01)
Single leg drop jump	**BTB n=48**	**HS n=62**	**Controls n=123**	**p value**	**d**	**Mean difference (95% CIs)**	**p value**	**d**	**Mean difference (95% CIs)**	**p value**	**d**	**Mean difference (95% CIs)**
Eccentric impulse	95±7	96±8	100±8	0.60		-1.5 (-5.0, 2.1)	**0.002**	0.58	-4.6 (-7.7, -1.5)	**0.029**	0.39	-3.1 (-6.0, -0.3)
Force at zero velocity	88±12	95±10	101±11	**0.003**	0.64	-6.9 (-11.8, -2.0)	**<0.001**	1.17	-13.1 (-17.5, -8.8)	**0.001**	0.60	-6.2 (-10.2, -2.3)
Concentric impulse	91±6	93±7	101±6	0.23		-2.0 (-5.0, 0.9)	**<0.001**	1.60	-9.9 (-12.5, -7.3)	**<0.001**	1.20	-7.9 (-10.3, -5.5)
Peak landing force	100±11	96±11	100±14	0.28		3.7 (-2.0, 9.4)	0.95		0.7 (-4.4, 5.7)	0.27		-3.0 (-7.6, 1.6)
	BTB n=45	**HS n=43**	**Controls n=123**									
Jump height symmetry	83±11	89±12	102±13	0.06		-6.0 (-12.2, 0.2)	**<0.001**	1.53	-19.0 (-24.0, -13.9)	**<0.001**	1.03	-13.0 (-18.2, -7.8)
Contact time symmetry	108±15	104±11	100±10	0.23		4.1 (-1.8, 10.0)	**<0.001**	0.72	8.4 (3.6, 13.2)	0.09		4.3 (-0.5, 9.2)
RSI symmetry	78±16	86±16	103±17	0.07		-8.0 (-16.5, 0.5)	**<0.001**	1.45	-24.8 (-31.7, -17.9)	**<0.001**	0.99	-16.8 (-23.9, -9.8)

Supplementary file 3

Table. Comparison of performance metrics between professional athletes in the ACLR and control group.

PERFORMANCE METRICS-BILATERAL							
Countermovement jump	**Professional ACLR n=94**		**Controls n=532**				
	Mean±SD	**CV%**	**Mean±SD**	**CV%**	**p value**	**d**	**Mean difference (95% CIs)**
Jump height	33.34±5.02	16.29	36.30±5.43	13.64	**<0.001**	-0.55	-2.96 (-4.14, -1.78)
Drop jump	**Professional ACLR n=43**		**Controls n=100**		**p value**	**d**	**Mean difference (95% CIs)**
Jump height	35.89±5.92	16.50	36.05±4.93	13.69	0.87		-0.16 (-2.05, 1.73)
Contact time	0.39±0.12	31.63	0.34±0.13	37.57	**0.014**	0.42	0.05 (0.008, 0.10)
RSI	1.09±0.29	26.74	1.38±0.55	39.78	**0.002**	-0.60	-0.29 (-0.43, -0.15)

PERFORMANCE METRICS-UNILATERAL															
								INVOLVED-UNINVOLVED			**INVOLVED-CONTROLS**			**UNINVOLVED-CONTROLS**		
Single leg jump	**Professional ACLR INVOLVED n=86**		**Professional ACLR UNINVOLVED n=86**		**Controls n=516**											
	Mean±SD	**CV%**	**Mean±SD**	**CV%**	**Mean±SD**	**CV%**		**p value**	**d**	**Mean difference (95% CIs)**	**p value**	**d**	**Mean difference (95% CIs)**	**p value**	**d**	**Mean difference (95% CIs)**
Jump height	14.23±3.41	23.9	16.49±3.34	20.2	17.44±3.66	21.0		**<0.001**	0.67	-2.26 (-3.54, -0.97)	**<0.001**	0.89	-3.21 (-4.19, -2.22)	0.06		-0.95 (-1.93, 0.03)
Single leg drop jump	**Professional ACLR INVOLVED n=88**		**Professional ACLR UNINVOLVED n=88**		**Controls n=123**			**p value**	**d**	**Mean difference (95% CIs)**	**p value**	**d**	**Mean difference (95% CIs)**	**p value**	**d**	**Mean difference (95% CIs)**
Jump height	14.61±3.49	23.9	17.09±3.63	21.2	18.45±2.92	15.8		**<0.001**	0.70	-2.47 (-3.65, -1.30)	**<0.001**	1.21	-3.84 (-4.93, -2.75)	**0.01**	0.42	-1.36 (-2.45, -0.28)
Contact time	0.41±0.10	23.6	0.38±0.09	22.3	0.33±0.07	21.2		0.20		0.02 (-0.01, 0.05)	**<0.001**	0.95	007 (0.05, 0.10)	**<0.001**	0.63	0.05 (0.03, 0.08)
RSI	0.38±0.12	30.8	0.47±0.14	30.8	0.58±0.13	22.4		**<0.001**	0.69	-0.09 (-0.14, -0.04)	**<0.001**	1.59	-0.20 (-0.24, -0.16)	**<0.001**	0.82	-0.10 (-0.15, -0.07)

Supplementary file 4

Table. Exploratory comparison of all metrics (mean±SD) between all patients after ACLR and control group.

Countermovement jump

	ACLR n=126	Controls n=532	p value	d	Mean difference (95% CIs)
START_OF_MOVEMENT	16.45±6.88	12.81±6.77	**<0.001**	0.534	3.63 (2.31, 4.96)
START_OF_MOVEMENT_THRESHOLD	18.44±1.02	18.29±1	0.132		0.15 (-0.04, 0.34)
START_OF_INTEGRATION	16.45±6.88	12.81±6.77	**<0.001**	0.534	3.63 (2.31, 4.96)
BEGIN_CONCENTRIC_PHASE	17±6.89	13.38±6.76	**<0.001**	0.532	3.62 (2.3, 4.94)
COUNTERMOVEMENT_DEPTH	-34.6±5.81	-33.3±6.91	0.051		-1.3 (-2.61, 0)
BODYMASS_RELATIVE_TAKEOFF_POWER	46.52±6.42	50.74±5.87	**<0.001**	-0.705	-4.22 (-5.39, -3.06)
FLIGHT_TIME	0.51±0.05	0.54±0.04	**<0.001**	-0.786	-0.03 (-0.04, -0.02)
JUMP_HEIGHT	31.61±5.97	35.48±4.93	**<0.001**	-0.751	-3.87 (-4.87, -2.87)
JUMP_HEIGHT_RELATIVE_LANDING_RFD	1757.2±1009	3089.6±2317.2	**<0.001**	-0.625	-1332.46 (-1747, -917.93)
JUMP_HEIGHT_RELATIVE_PEAK_LANDING_FORCE	109.18±35.94	141.56±42.1	**<0.001**	-0.789	-32.38 (-40.36, -24.4)
IMPULSE_JUMP_HEIGHT	31.08±5.61	35.01±5.25	**<0.001**	-0.736	-3.92 (-4.96, -2.89)
JUMP_HEIGHT_IMP_MOM	31.07±5.61	35.01±5.25	**<0.001**	-0.739	-3.94 (-4.98, -2.91)
LANDING_RFD	55586±35499	111212±92870	**<0.001**	-0.654	-55625.77 (-72158.12, -39093.41)
JUMP_HEIGHT_INCHES	12.45±2.35	13.97±1.94	**<0.001**	-0.751	-1.52 (-1.92, -1.13)
JUMP_HEIGHT_INCHES_IMP_MOM	12.23±2.21	13.79±2.07	**<0.001**	-0.739	-1.55 (-1.96, -1.14)
MEAN_LANDING_ACCELERATION	2.56±0.39	2.67±0.4	**0.008**	-0.263	-0.1 (-0.18, -0.03)
MEAN_LANDING_POWER	676.84±227.26	581.5±165.43	**<0.001**	0.532	95.34 (60.54, 130.13)
MEAN_LANDING_VELOCITY	-0.13±0.16	-0.1±0.16	0.062		-0.03 (-0.06, 0)
MEAN_TAKEOFF_ACCELERATION	8.56±1.53	9.57±1.7	**<0.001**	-0.604	-1.01 (-1.33, -0.68)
MEAN_TAKEOFF_FORCE	1417.7±242.84	1430.5±217.92	0.563		-12.79 (-56.15, 30.57)
MEAN_ECCENTRIC_FORCE	760.03±130.37	725.85±98.74	**0.001**	0.324	34.18 (13.65, 54.7)
MEAN_ECCENTRIC_POWER	482.26±122.4	434.21±118.66	**<0.001**	0.402	48.05 (24.82, 71.27)
MEAN_ECC_CON_RATIO	53.82±4.27	51.08±4.34	**<0.001**	0.633	2.74 (1.9, 3.58)
MEAN_CONCENTRIC_POWER	1955.7±384.33	2056.1±386.28	**0.009**	-0.260	-100.34 (-175.41, -25.26)
BODYMASS_RELATIVE_MEAN_CONCENTRIC_POWER	25.37±3.52	27.83±3.68	**<0.001**	-0.673	-2.46 (-3.17, -1.75)
BODYMASS_RELATIVE_MEAN_ECCENTRIC_POWER	6.22±1.12	5.86±1.32	**0.005**	0.276	0.35 (0.11, 0.6)
MEAN_TAKEOFF_VELOCITY	1.51±0.12	1.56±0.12	**<0.001**	-0.426	-0.05 (-0.08, -0.03)
PEAK_LANDING_ACCELERATION	34.2±12.8	57.78±19.73	**<0.001**	**-1.265**	-23.58 (-27.2, -19.96)
PEAK_LANDING_FORCE	3348.7±916	4968.9±1484	**<0.001**	**-1.161**	-1620.15 (-1891.29, -1349.01)
PEAK_LANDING_POWER	6467.3±2228.2	9739.8±3582.4	**<0.001**	**-0.971**	-3272.52 (-3927.48, -2617.56)
PEAK_LANDING_VELOCITY	0.7±0.26	0.67±0.23	0.197		0.03 (-0.02, 0.08)
PEAK_TAKEOFF_ACCELERATION	12.81±2.14	13.85±2.56	**<0.001**	-0.416	-1.03 (-1.52, -0.55)
PEAK_TAKEOFF_FORCE	1750.3±323	1747.8±290.41	0.934		2.44 (-55.32, 60.2)
PEAK_TAKEOFF_POWER	3581.1±681.83	3750.8±674.04	**0.011**	-0.251	-169.69 (-301.11, -38.26)
PEAK_TAKEOFF_VELOCITY	2.6±0.2	2.73±0.19	**<0.001**	-0.685	-0.13 (-0.17, -0.09)
CONCENTRIC_RFD	1431±1002.9	1806.2±1456.9	**0.006**	-0.271	-375.23 (-644.08, -106.37)
CONCENTRIC_RFD_100	-1083±1809.6	-339.4±2205.6	**<0.001**	-0.348	-743.94 (-1159.46, -328.42)
CONCENTRIC_RFD_200	-1202±2315.1	-1376±2574.5	0.487		174.2 (-317.44, 665.85)
CONCENTRIC_RFD_50	-338.8±1925	505.46±2288.7	**<0.001**	-0.379	-844.29 (-1276.95, -411.63)
TIME_TO_PEAK_FORCE	0.07±0.07	0.09±0.08	0.051		-0.01 (-0.03, 0)
CONTRACTION_TIME	0.85±0.1	0.85±0.15	0.751		0 (-0.03, 0.02)
ECCENTRIC_TIME	0.55±0.08	0.57±0.12	0.115		-0.02 (-0.04, 0)
START_TO_PEAK_FORCE_TIME	0.62±0.12	0.65±0.17	**0.044**	-0.199	-0.03 (-0.06, 0)
START_TO_PEAK_POWER_TIME	0.78±0.1	0.79±0.15	0.557		-0.01 (-0.04, 0.02)
WEIGHT_RELATIVE_PEAK_LANDING_FORCE	34.2±12.8	57.78±19.73	**<0.001**	**-1.265**	-23.58 (-27.2, -19.96)
WEIGHT_RELATIVE_PEAK_TAKEOFF_FORCE	12.83±2.15	13.86±2.56	**<0.001**	-0.413	-1.03 (-1.51, -0.55)
RELATIVE_CONCENTRIC_RFD	18.9±13.18	24.93±21.55	**0.003**	-0.298	-6.03 (-9.96, -2.09)
CONCENTRIC_DURATION	0.29±0.04	0.28±0.05	**0.003**	0.299	0.01 (0, 0.02)

CONCENTRIC_ECCENTRIC_DURATION_RATIO	153.46±6.54	150.36±8.15	**<0.001**	0.393	3.1 (1.57, 4.63)
ECCENTRIC_CONCENTRIC_DURATION_RATIO	190.72±25.55	205.39±32.88	**<0.001**	-0.463	-14.67 (-20.82, -8.52)
FLIGHT_CONTRACTION_TIME_RATIO	0.61±0.1	0.65±0.12	**<0.001**	-0.374	-0.04 (-0.07, -0.02)
FLIGHT_ECCENTRIC_TIME_RATIO	0.94±0.16	0.99±0.2	**0.009**	-0.258	-0.05 (-0.09, -0.01)
BEGIN_BRAKING_PHASE	16.63±6.89	13±6.77	**<0.001**	0.533	3.63 (2.3, 4.95)
MIN_ECCENTRIC_FORCE	276.99±130.94	289.87±147.65	0.369		-12.88 (-41.01, 15.26)
BRAKING_PHASE_DURATION	0.37±0.06	0.38±0.1	0.393		-0.01 (-0.03, 0.01)
BEGIN_ECC_DECEL_PHASE	16.79±6.88	13.17±6.77	**<0.001**	0.532	3.62 (2.3, 4.94)
TIME_TO_BRAKING_PHASE	0.18±0.04	0.19±0.05	0.082		-0.01 (-0.02, 0)
ECCENTRIC_ACCEL_PHASE_DURATION	0.35±0.06	0.36±0.08	0.051		-0.01 (-0.03, 0)
ECCENTRIC_DECEL_PHASE_DURATION	0.21±0.04	0.21±0.06	0.792		0 (-0.01, 0.01)
BEAKING_CONTRACTION_DURATION_RATIO	43.64±3.99	43.91±5.29	0.584		-0.28 (-1.26, 0.71)
BEAKING_CONCENTRIC_DURATION_RATIO	127.2±18.3	134.8±25.99	**0.002**	-0.307	-7.59 (-12.4, -2.79)
MEAN_ECCENTRIC_BRAKING_FORCE	890.01±159.01	849.63±128.89	**0.003**	0.298	40.38 (14.09, 66.68)
MEAN_ECCENTRIC_DECELERATION_FORCE	1228.1±254.24	1167.4±231.16	**0.010**	0.257	60.68 (14.82, 106.54)
FORCE_AT_PEAK_POWER	1525.8±259.94	1530±237.15	0.862		-4.16 (-51.17, 42.86)
CONCENTRIC_IMPULSE_50MS	45.31±12.12	45.27±12.63	0.977		0.04 (-2.4, 2.47)
CONCENTRIC_IMPULSE_100MS	87.11±22.22	89±22.7	0.398		-1.89 (-6.29, 2.51)
CONCENTRIC_IMPULSE_P1	119.81±23.16	118.3±20.44	0.468		1.51 (-2.57, 5.59)
CONCENTRIC_IMPULSE_P2	69.94±16.65	74.99±17.21	**0.003**	-0.295	-5.05 (-8.38, -1.72)
ECCENTRIC_BRAKING_RFD	3991.7±1544.5	3956.5±1932.3	0.849		35.23 (-327.52, 397.99)
RELATIVE_ECCENTRIC_BRAKING_RFD	51.47±18.02	53.7±25.46	0.353		-2.23 (-6.94, 2.48)
ECCENTRIC_BRAKING_RFD_100MS	2622.7±1393.8	2578.9±1746.5	0.793		43.74 (-284.07, 371.56)
RELATIVE_ECCENTRIC_BRAKING_RFD_100MS	33.85±17.21	34.98±23.16	0.606		-1.13 (-5.44, 3.18)
ECCENTRIC_DECEL_RFD	4736.4±2008.2	4930±2567.3	0.429		-193.59 (-674.21, 287.04)
RELATIVE_ECCENTRIC_DECEL_RFD	61.03±23.28	67.06±34.45	0.063		-6.03 (-12.37, 0.32)
RELATIVE_PEAK_TAKEOFF_FORCE	22.64±2.15	23.67±2.56	**<0.001**	-0.413	-1.03 (-1.51, -0.54)
PEAK_CONCENTRIC_FORCE	1748.5±321.66	1746.6±289.95	0.948		1.9 (-55.73, 59.54)
RELATIVE_PEAK_CONCENTRIC_FORCE	22.62±2.14	23.65±2.56	**<0.001**	-0.416	-1.03 (-1.52, -0.55)
PEAK_ECCENTRIC_FORCE	1663.6±346.82	1606.3±320.07	0.076		57.29 (-6, 120.59)
RELATIVE_PEAK_ECCENTRIC_FORCE	21.48±2.58	21.75±3.3	0.393		-0.27 (-0.89, 0.35)
RELATIVE_PEAK_LANDING_FORCE	44.01±12.8	67.58±19.73	**<0.001**	**-1.265**	-23.58 (-27.2, -19.96)
MEAN_ECC_CON_POWER_TIME	1206.9±329.93	1204.8±367	0.954		2.06 (-68.02, 72.14)
LOWER_LIMB_STIFFNESS	4098.6±1260.7	4201.5±1641.4	0.510		-102.98 (-409.58, 203.62)
CONCENTRIC_RPD	16579±5165.3	18337±5850.8	**0.002**	-0.307	-1757.53 (-2871.6, -643.47)
RELATIVE_CONCENTRIC_RPD	215.99±62.49	249.1±76.12	**<0.001**	-0.449	-33.11 (-47.45, -18.77)
CONCENTRIC_RPD_50MS	19621±7209.1	20574±8300.8	0.236		-952.63 (-2529.25, 623.98)
RELATIVE_CONCENTRIC_RPD_50MS	254.08±84.17	279.62±110.3	**0.015**	-0.241	-25.53 (-46.12, -4.95)
CONCENTRIC_RPD_100MS	17766±6222.5	19312±6683	**0.018**	-0.234	-1546.27 (-2829.83, -262.7)
RELATIVE_CONCENTRIC_RPD_100MS	230.58±73.81	262.43±87.52	**<0.001**	-0.374	-31.84 (-48.39, -15.29)
RSI_MODIFIED	38.19±9.32	43.23±9.46	**<0.001**	-0.534	-5.04 (-6.87, -3.2)
TOTAL_WORK	832.6±180.25	813.75±172.94	0.276		18.85 (-15.07, 52.77)
VELOCITY_AT_PEAK_POWER	2.35±0.19	2.45±0.18	**<0.001**	-0.570	-0.1 (-0.14, -0.07)
ECCENTRIC_PEAK_VELOCITY	-1.18±0.23	-1.11±0.27	**0.016**	-0.239	-0.06 (-0.11, -0.01)
ECCENTRIC_PEAK_POWER	1169.5±392	1065.1±408.49	**0.010**	0.257	104.35 (25.48, 183.22)
ECCENTRIC_BRAKING_IMPULSE	45.02±13.25	41.18±13.37	**0.004**	0.287	3.84 (1.24, 6.43)
ECCENTRIC_DECEL_IMPULSE	91.25±24.3	82.54±23.96	**<0.001**	0.362	8.71 (4.03, 13.38)
CONCENTRIC_IMPULSE	189.75±33.43	193.29±31.06	0.258		-3.54 (-9.67, 2.59)
FORCE_AT_ZERO_VELOCITY	1659.2±347.16	1603.3±319.6	0.083		55.92 (-7.31, 119.15)
POSITIVE_IMPULSE	533.75±106.32	524.34±93.12	0.321		9.41 (-9.22, 28.05)
ECCENTRIC_UNLOADING_IMPULSE	-91.25±24.31	-82.55±23.94	**<0.001**	-0.362	-8.7 (-13.37, -4.03)
POSITIVE_TAKEOFF_IMPULSE	292.28±55.63	284.63±49.77	0.130		7.64 (-2.27, 17.55)
CMJ_STIFFNESS	5228.2±1421	5882.1±3547.9	**0.043**	-0.201	-653.9 (-1286.52, -21.28)
CONCENTRIC_RFD_MAX	2806.6±1595.7	3238.3±1840.1	0.080		-431.7 (-915.68, 52.29)
TAKEOFF_VELOCITY	2.46±0.22	2.61±0.2	**<0.001**	-0.763	-0.15 (-0.19, -0.11)
BODYMASS_RELATIVE_MEAN_TAKEOFF_FORCE	18.37±1.53	19.38±1.7	**<0.001**	-0.604	-1.01 (-1.33, -0.68)
BODYMASS_RELATIVE_ECCENTRIC_PEAK_POWER	15.05±4.24	14.36±4.92	0.145		0.69 (-0.24, 1.63)
ECC_CON_PEAK_POWER_RATIO	0.33±0.09	0.29±0.1	**<0.001**	0.414	0.04 (0.02, 0.06)
CON_P2_CON_P1_IMPULSE_RATIO	0.6±0.17	0.65±0.16	**0.003**	-0.295	-0.05 (-0.08, -0.02)

CON_100MS_CON_IMPULSE_RATIO	0.46±0.09	0.46±0.11	0.702		0 (-0.02, 0.02)
LANDING_IMPULSE	106.81±32.5	101.11±30.03	0.060		5.7 (-0.23, 11.64)
LANDING_RFD_50	41124±15482	64119±25878	**<0.001**	**-0.947**	-22994.46 (-27710.89, -18278.02)
INV_LANDING_RFD	30401±21804	60986±53019	**<0.001**	-0.628	-30585.17 (-40048.06, -21122.28)
INV_MEAN_TAKEOFF_FORCE	680.27±119.72	711.33±113.66	**0.006**	-0.270	-31.06 (-53.41, -8.72)
INV_MEAN_ECCENTRIC_FORCE	376.79±71.25	357.24±54.77	**0.001**	0.335	19.54 (8.21, 30.88)
INV_MEAN_ECC_CON_RATIO	55.6±5.47	50.58±5.25	**<0.001**	**0.947**	5.02 (3.99, 6.05)
INV_PEAK_LANDING_FORCE	1689±522.32	2649.9±816.49	**<0.001**	**-1.248**	-960.91 (-1110.55, -811.27)
INV_PEAK_TAKEOFF_FORCE	854.24±162.1	871.27±150.94	0.262		-17.03 (-46.82, 12.76)
INV_CONCENTRIC_RFD	706.55±729.24	995.71±880.54	**0.001**	-0.336	-287.26 (-455.97, -118.54)
INV_FORCE_AT_PEAK_POWER	724.74±126.06	764.09±121.72	**0.001**	-0.321	-39.34 (-63.19, -15.5)
INV_CONCENTRIC_IMPULSE_50MS	40.49±8.31	40.19±8.05	0.712		0.3 (-1.28, 1.87)
INV_CONCENTRIC_IMPULSE_100MS	79.19±15.53	79.82±14.86	0.671		-0.63 (-3.55, 2.29)
INV_CONCENTRIC_IMPULSE_P1	112.17±22.21	108.86±19.01	0.089		3.32 (-0.51, 7.14)
INV_CONCENTRIC_IMPULSE_P2	85.92±18.72	88.55±18.98	0.161		-2.63 (-6.32, 1.05)
INV_ECCENTRIC_BRAKING_RFD	1936.1±750.39	1977.2±979.41	0.659		-41.08 (-223.97, 141.81)
INV_ECCENTRIC_BRAKING_RFD_100MS	1351.2±758.33	1326.4±922.82	0.779		24.86 (-149.03, 198.75)
INV_ECCENTRIC_DECEL_RFD	2267.7±962.74	2447.7±1314.7	0.148		-180.07 (-424.27, 64.14)
INV_PEAK_CONCENTRIC_FORCE	852.7±161.41	870.18±150.46	0.248		-17.48 (-47.17, 12.21)
INV_PEAK_ECCENTRIC_FORCE	810.39±174.61	791.69±168.36	0.266		18.69 (-14.3, 51.68)
INV_ECCENTRIC_BRAKING_IMPULSE	159.88±36.01	154.45±42.6	0.186		5.43 (-2.63, 13.49)
INV_ECCENTRIC_DECEL_IMPULSE	120.07±26.26	113.9±28.57	0.027		6.18 (0.7, 11.65)
INV_CONCENTRIC_IMPULSE	198.09±39.52	197.41±36.25	0.852		0.68 (-6.49, 7.86)
INV_FORCE_AT_ZERO_VELOCITY	807.33±173.72	788.54±168.56	0.264		18.79 (-14.2, 51.77)
INV_POSITIVE_IMPULSE	601.37±147.65	523.4±115.37	**<0.001**	0.637	77.96 (54.19, 101.73)
INV_ECCENTRIC_UNLOADING_IMPULSE	87.6±31.61	89.86±40.09	0.554		-2.26 (-9.78, 5.25)
INV_POSITIVE_TAKEOFF_IMPULSE	314.69±63.36	306.87±61.29	0.201		7.81 (-4.19, 19.82)
INV_CMJ_STIFFNESS	2551.2±704.41	2932.9±1795.2	**0.019**	-0.232	-381.72 (-701.58, -61.87)
INV_CONCENTRIC_RFD_MAX	1402.4±872.56	1814.4±1015.2	**0.003**	-0.414	-411.92 (-678.63, -145.2)
INV_CONCENTRIC_RFD_100	-553.8±930.23	-94.1±1145.6	**<0.001**	-0.414	-459.69 (-675.21, -244.16)
INV_CONCENTRIC_RFD_200	-640.4±1124.7	-625.3±1285.1	0.904		-15.08 (-259.45, 229.29)
INV_CONCENTRIC_RFD_50	-195.9±999.15	327.91±1213.8	**<0.001**	-0.445	-523.77 (-752.6, -294.95)
INV_CON_P2_CON_P1_IMPULSE_RATIO	0.77±0.09	0.81±0.1	**<0.001**	-0.462	-0.05 (-0.07, -0.03)
INV_CON_100MS_CON_IMPULSE_RATIO	0.41±0.07	0.41±0.09	0.370		-0.01 (-0.02, 0.01)
INV_LANDING_IMPULSE	48.02±18.03	49.44±16.05	0.383		-1.42 (-4.62, 1.78)
UNINV_LANDING_RFD	33734±23355	61487±56853	**<0.001**	-0.532	-27753.22 (-37900.06, -17606.38)
UNINV_MEAN_TAKEOFF_FORCE	737.45±129.72	719.17±110.01	0.106		18.27 (-3.91, 40.46)
UNINV_MEAN_ECCENTRIC_FORCE	383.24±67.92	368.61±53.68	**0.009**	0.258	14.64 (3.61, 25.66)
UNINV_MEAN_ECC_CON_RATIO	52.27±5.23	51.63±5.28	0.221		0.64 (-0.39, 1.67)
UNINV_PEAK_LANDING_FORCE	1914.4±534.59	2667±861.62	**<0.001**	-0.929	-752.56 (-910.05, -595.06)
UNINV_PEAK_TAKEOFF_FORCE	907.13±169.62	888.19±147.51	0.209		18.94 (-10.63, 48.5)
UNINV_CONCENTRIC_RFD	771.38±588.27	848.48±835.21	0.345		-75.47 (-232.39, 81.45)
UNINV_FORCE_AT_PEAK_POWER	801.09±140.13	765.9±119.47	**0.004**	0.284	35.19 (11.13, 59.25)
UNINV_CONCENTRIC_IMPULSE_50MS	42.78±9.02	41.33±7.88	0.072		1.45 (-0.13, 3.03)
UNINV_CONCENTRIC_IMPULSE_100MS	83.84±17.02	81.69±14.59	0.150		2.15 (-0.78, 5.09)
UNINV_CONCENTRIC_IMPULSE_P1	118.83±23.04	111.07±18.16	**<0.001**	0.404	7.76 (4.03, 11.49)
UNINV_CONCENTRIC_IMPULSE_P2	95.59±19.89	88.43±18.63	**<0.001**	0.379	7.16 (3.49, 10.83)
UNINV_ECCENTRIC_BRAKING_RFD	2084.8±813.38	2020.9±993.98	0.503		63.89 (-123.3, 251.08)
UNINV_ECCENTRIC_BRAKING_RFD_100MS	1368.6±744.35	1391.9±925.57	0.793		-23.3 (-197.2, 150.6)
UNINV_ECCENTRIC_DECEL_RFD	2468.7±1129.6	2482.2±1311.1	0.915		-13.52 (-262.25, 235.21)
UNINV_PEAK_CONCENTRIC_FORCE	905.79±168.33	887.08±147.28	0.213		18.71 (-10.76, 48.19)
UNINV_PEAK_ECCENTRIC_FORCE	855.86±185.86	817.64±165.03	**0.023**	0.226	38.22 (5.3, 71.14)
UNINV_ECCENTRIC_BRAKING_IMPULSE	165.74±35.86	161.75±43.35	0.339		3.99 (-4.19, 12.16)
UNINV_ECCENTRIC_DECEL_IMPULSE	126.51±27.53	118.75±28.41	**0.006**	0.275	7.77 (2.27, 13.26)
UNINV_CONCENTRIC_IMPULSE	214.42±41.02	199.5±34.95	**<0.001**	0.412	14.92 (7.88, 21.96)
UNINV_FORCE_AT_ZERO_VELOCITY	851.91±186.74	814.78±165	**0.027**	0.219	37.13 (4.18, 70.08)
UNINV_POSITIVE_IMPULSE	638.51±148.23	535.36±110.99	**<0.001**	**0.866**	103.15 (80, 126.3)
UNINV_ECCENTRIC_UNLOADING_IMPULSE	85.08±32.3	91.74±41.7	0.094		-6.66 (-14.46, 1.13)
UNINV_POSITIVE_TAKEOFF_IMPULSE	336.03±66.22	314.13±59.45	**<0.001**	0.360	21.9 (10.07, 33.72)

UNINV_CMJ_STIFFNESS	2709.6±734.86	2986±1769.6	0.086		-276.35 (-592.3, 39.61)
UNINV_CONCENTRIC_RFD_MAX	1606.4±994.5	1633.3±1011.3	0.846		-26.82 (-297.54, 243.9)
UNINV_CONCENTRIC_RFD_100	-529.5±968.16	-245.3±1151	**0.011**	-0.254	-284.25 (-501.85, -66.66)
UNINV_CONCENTRIC_RFD_200	-561.4±1231.8	-750.7±1327.5	0.145		189.28 (-65.53, 444.1)
UNINV_CONCENTRIC_RFD_50	-143±1061.8	177.55±1217.7	**0.007**	-0.269	-320.52 (-552, -89.03)
UNINV_CON_P2_CON_P1_IMPULSE_RATIO	0.81±0.1	0.8±0.1	0.179		0.01 (-0.01, 0.03)
UNINV_CON_100MS_CON_IMPULSE_RATIO	0.4±0.07	0.42±0.09	**0.006**	-0.270	-0.02 (-0.04, -0.01)
UNINV_LANDING_IMPULSE	55.54±18.85	49.68±16.03	**<0.001**	0.353	5.86 (2.63, 9.09)
LSI.LANDING_RFD	94.84±37.74	105.16±33.15	**0.002**	-0.303	-10.32 (-16.95, -3.69)
LSI.MEAN_TAKEOFF_FORCE	92.51±7.37	99.05±6.79	**<0.001**	**-0.946**	-6.54 (-7.88, -5.2)
LSI.MEAN_ECCENTRIC_FORCE	98.92±12.47	97.54±12.17	0.255		1.38 (-1, 3.76)
LSI.MEAN_ECC_CON_RATIO	107.19±12.89	98.62±11.5	**<0.001**	0.727	8.57 (6.28, 10.86)
LSI.PEAK_LANDING_FORCE	89.83±20.15	101.43±19.05	**<0.001**	-0.601	-11.6 (-15.35, -7.85)
LSI.PEAK_TAKEOFF_FORCE	94.42±8.15	98.27±7.56	**<0.001**	-0.501	-3.85 (-5.34, -2.35)
LSI.CONCENTRIC_RFD	-43.2±1787.7	57.99±3507	0.757		-101.19 (-743.67, 541.28)
LSI.FORCE_AT_PEAK_POWER	90.7±6.6	99.87±5.52	**<0.001**	**-1.595**	-9.17 (-10.29, -8.06)
LSI.CONCENTRIC_IMPULSE_50MS	95.35±10.66	97.62±10.46	**0.029**	-0.216	-2.27 (-4.31, -0.23)
LSI.CONCENTRIC_IMPULSE_100MS	95.05±9.54	98±9.14	**0.001**	-0.320	-2.96 (-4.75, -1.16)
LSI.CONCENTRIC_IMPULSE_P1	94.7±8.48	98.18±8.24	**<0.001**	-0.419	-3.48 (-5.09, -1.86)
LSI.CONCENTRIC_IMPULSE_P2	90.02±8.08	100.32±7.02	**<0.001**	**-1.423**	-10.31 (-11.71, -8.9)
LSI.ECCENTRIC_BRAKING_RFD	95.34±18.62	100.35±21.16	**0.015**	-0.242	-5.02 (-9.04, -0.99)
LSI.ECCENTRIC_BRAKING_RFD_100MS	109.5±53.86	108.56±63.25	0.878		0.94 (-11.04, 12.92)
LSI.ECCENTRIC_DECEL_RFD	97.19±29.51	101.49±23.63	0.081		-4.31 (-9.14, 0.53)
LSI.PEAK_CONCENTRIC_FORCE	94.38±8.11	98.27±7.51	**<0.001**	-0.509	-3.89 (-5.37, -2.41)
LSI.PEAK_ECCENTRIC_FORCE	95.37±11.25	97.3±11.59	0.092		-1.93 (-4.17, 0.31)
LSI.ECCENTRIC_BRAKING_IMPULSE	97.38±14.17	96.36±14.68	0.481		1.02 (-1.82, 3.86)
LSI.ECCENTRIC_DECEL_IMPULSE	95.71±12.86	96.63±14.38	0.513		-0.91 (-3.66, 1.83)
LSI.CONCENTRIC_IMPULSE	92.51±7.35	99.04±6.78	**<0.001**	**-0.947**	-6.53 (-7.87, -5.19)
LSI.FORCE_AT_ZERO_VELOCITY	95.54±11.44	97.27±11.8	0.139		-1.72 (-4, 0.56)
LSI.POSITIVE_IMPULSE	94.47±10.97	98.03±10.42	**0.001**	-0.338	-3.56 (-5.61, -1.51)
LSI.ECCENTRIC_UNLOADING_IMPULSE	105.58±21.16	100.64±21.5	**0.020**	0.230	4.94 (0.77, 9.11)
LSI.POSITIVE_TAKEOFF_IMPULSE	93.92±8.34	97.86±8.69	**<0.001**	-0.457	-3.95 (-5.63, -2.27)
LSI.CMJ_STIFFNESS	94.41±8.15	98.27±7.53	**<0.001**	-0.503	-3.86 (-5.35, -2.37)
LSI.CONCENTRIC_RFD_MAX	116.21±148.31	92.45±587.02	0.748		23.77 (-121.52, 169.05)
LSI.CONCENTRIC_RFD_100	144.9±1724.3	109.89±434.31	0.677		35.01 (-129.98, 200)
LSI.CONCENTRIC_RFD_200	68.13±768.56	87.44±468.53	0.718		-19.3 (-124.11, 85.5)
LSI.CONCENTRIC_RFD_50	1166.5±13230	34.47±961.14	0.051		1132.06 (-6.13, 2270.25)
LSI.CON_P2_CON_P1_IMPULSE_RATIO	95.34±8.2	102.62±7.63	**<0.001**	**-0.940**	-7.28 (-8.79, -5.78)
LSI.CON_100MS_CON_IMPULSE_RATIO	102.73±5.18	98.79±4.5	**<0.001**	**0.846**	3.93 (3.03, 4.84)
LSI.LANDING_IMPULSE	89.13±24.79	102.08±24.32	**<0.001**	-0.530	-12.95 (-17.7, -8.2)

Single leg jump

	ACLR n=118	Controls n=516	p value	d	Mean difference (95% CIs)
INV_START_OF_MOVEMENT	13.62±5.41	11.08±5.44	**<0.001**	0.468	2.55 (1.46, 3.64)
INV_START_OF_MOVEMENT_THRESHOLD	18.39±0.93	18.53±4.74	0.754		-0.14 (-1, 0.72)
INV_BEGIN_CONCENTRIC_PHASE	14.16±5.4	11.6±5.45	**<0.001**	0.469	2.56 (1.47, 3.65)
INV_COUNTERMOVEMENT_DEPTH	-20.69±5.49	-19.88±6.37	0.203		-0.81 (-2.05, 0.44)
INV_BODYMASS_RELATIVE_TAKEOFF_POWER	26.84±4.28	32.02±4.08	**<0.001**	**-1.255**	-5.17 (-6, -4.35)
INV_FLIGHT_TIME	0.33±0.05	0.38±0.04	**<0.001**	**-1.404**	-0.05 (-0.06, -0.05)
INV_JUMP_HEIGHT	13.32±3.89	17.88±3.31	**<0.001**	**-1.328**	-4.56 (-5.24, -3.87)
INV_JUMP_HEIGHT_RELATIVE_LANDING_RFD	2695.3±1285.2	3132.3±2330.8	0.049	-0.201	-436.91 (-872.84, -0.98)
INV_JUMP_HEIGHT_RELATIVE_PEAK_LANDING_FORCE	200.65±66.57	169.64±38.41	**<0.001**	0.689	31.01 (22, 40.02)
INV_IMPULSE_JUMP_HEIGHT	12.68±3.68	17.23±3.52	**<0.001**	**-1.281**	-4.56 (-5.27, -3.84)
INV_JUMP_HEIGHT_IMP_MOM	12.67±3.68	17.24±3.52	**<0.001**	**-1.283**	-4.57 (-5.28, -3.85)
INV_LANDING_RFD	34602±19683	56703±46965	**<0.001**	-0.511	-22101.82 (-30764.93, -13438.7)
INV_MEAN_LANDING_ACCELERATION	1.53±0.61	1.87±0.52	**<0.001**	-0.636	-0.34 (-0.45, -0.23)
INV_MEAN_LANDING_POWER	412.25±162.29	416.08±111.09	0.758		-3.84 (-28.32, 20.65)
INV_MEAN_LANDING_VELOCITY	-0.17±0.25	-0.12±0.18	**0.012**	-0.258	-0.05 (-0.09, -0.01)
INV_MEAN_TAKEOFF_ACCELERATION	4.75±1.07	5.75±1.31	**<0.001**	-0.784	-1 (-1.25, -0.74)
INV_MEAN_TAKEOFF_FORCE	1119.7±188.22	1148.8±174.33	0.107		-29.12 (-64.58, 6.35)
INV_MEAN_ECCENTRIC_FORCE	756.58±127.55	726.22±98.21	**0.004**	0.291	30.37 (9.47, 51.26)
INV_MEAN_ECCENTRIC_POWER	298.04±100.67	270.93±95.43	**0.006**	0.281	27.11 (7.79, 46.44)
INV_MEAN_ECC_CON_RATIO	67.79±4.95	63.65±5.34	**<0.001**	0.785	4.14 (3.09, 5.2)
INV_MEAN_CONCENTRIC_POWER	1084.1±237.56	1197.6±244.47	**<0.001**	-0.466	-113.49 (-162.23, -64.76)
INV_BODYMASS_RELATIVE_MEAN_CONCENTRIC_POWER	14.12±2.35	16.22±2.61	**<0.001**	**-0.819**	-2.1 (-2.62, -1.59)
INV_BODYMASS_RELATIVE_MEAN_ECCENTRIC_POWER	3.85±1.05	3.67±1.18	0.123		0.18 (-0.05, 0.42)
INV_MEAN_TAKEOFF_VELOCITY	1.05±0.12	1.12±0.13	**<0.001**	-0.492	-0.06 (-0.09, -0.04)
INV_PEAK_LANDING_ACCELERATION	22.67±6.89	30.39±7.11	**<0.001**	**-1.090**	-7.72 (-9.13, -6.3)
INV_PEAK_LANDING_FORCE	2469.4±517.23	2965.6±624	**<0.001**	**-0.818**	-496.21 (-617.57, -374.85)
INV_PEAK_LANDING_POWER	3588.9±1252.5	4859.1±1486.8	**<0.001**	**-0.877**	-1270.21 (-1560.01, -980.41)
INV_PEAK_LANDING_VELOCITY	0.39±0.29	0.46±0.21	**0.002**	-0.317	-0.07 (-0.12, -0.03)
INV_PEAK_TAKEOFF_ACCELERATION	8.29±1.63	9.89±2.06	**<0.001**	**-0.806**	-1.6 (-2, -1.21)
INV_PEAK_TAKEOFF_FORCE	1394.4±258.03	1456.9±249.04	**0.015**	-0.249	-62.46 (-112.7, -12.22)
INV_PEAK_TAKEOFF_POWER	2061.9±441.56	2367.5±444.65	**<0.001**	-0.687	-305.66 (-394.64, -216.67)
INV_PEAK_TAKEOFF_VELOCITY	1.81±0.19	2.01±0.17	**<0.001**	**-1.178**	-0.21 (-0.24, -0.17)
INV_CONCENTRIC_RFD	1045.8±722.09	1641.6±1139.6	**<0.001**	-0.554	-595.85 (-811.18, -380.51)
INV_CONCENTRIC_RFD_100	476.95±1116.9	847.02±1324.1	**0.005**	-0.287	-370.07 (-628.22, -111.92)
INV_CONCENTRIC_RFD_200	-57.45±1162.8	-71.96±2043.3	0.941		14.51 (-368.45, 397.48)
INV_CONCENTRIC_RFD_50	607.81±989.42	1066.6±1507.2	**0.002**	-0.321	-458.77 (-744.44, -173.1)
INV_CONCENTRIC_RFD_MAX	2433.3±1308.2	3299.3±1717.4	**<0.001**	-0.521	-866.05 (-1268.58, -463.51)
INV_TIME_TO_PEAK_FORCE	0.15±0.09	0.18±0.09	**0.001**	-0.334	-0.03 (-0.05, -0.01)
INV_CONTRACTION_TIME	0.87±0.14	0.86±0.17	0.491		0.01 (-0.02, 0.04)
INV_ECCENTRIC_TIME	0.54±0.1	0.53±0.13	0.477		0.01 (-0.02, 0.03)
INV_START_TO_PEAK_FORCE_TIME	0.68±0.17	0.71±0.19	0.224		-0.02 (-0.06, 0.01)
INV_START_TO_PEAK_POWER_TIME	0.77±0.14	0.77±0.17	0.925		0 (-0.03, 0.03)
INV_WEIGHT_RELATIVE_PEAK_LANDING_FORCE	22.67±6.89	30.39±7.11	**<0.001**	**-1.090**	-7.72 (-9.13, -6.3)
INV_WEIGHT_RELATIVE_PEAK_TAKEOFF_FORCE	8.3±1.63	9.9±2.06	**<0.001**	**-0.807**	-1.6 (-2, -1.21)
INV_RELATIVE_CONCENTRIC_RFD	13.59±8.99	22.24±14.91	**<0.001**	-0.617	-8.65 (-11.46, -5.84)
INV_CONCENTRIC_DURATION	0.34±0.05	0.33±0.08	0.730		0 (-0.01, 0.02)
INV_CONCENTRIC_ECCENTRIC_DURATION_RATIO	165.22±16.3	166.61±49.1	0.761		-1.39 (-10.39, 7.61)
INV_ECCENTRIC_CONCENTRIC_DURATION_RATIO	160.39±23.89	167.18±27.29	**0.013**	-0.254	-6.79 (-12.16, -1.42)
INV_FLIGHT_CONTRACTION_TIME_RATIO	0.39±0.09	0.47±0.11	**<0.001**	-0.761	-0.08 (-0.1, -0.06)
INV_FLIGHT_ECCENTRIC_TIME_RATIO	0.64±0.18	0.78±0.3	**<0.001**	-0.491	-0.14 (-0.2, -0.08)

INV_BEGIN_BRAKING_PHASE	13.8±5.41	11.25±5.44	**<0.001**	0.469	2.55 (1.47, 3.64)
INV_MIN_ECCENTRIC_FORCE	399.12±143.64	400.79±153.81	0.914		-1.67 (-32.13, 28.78)
INV_BRAKING_PHASE_DURATION	0.36±0.09	0.36±0.11	0.897		0 (-0.02, 0.02)
INV_BEGIN_ECC_DECEL_PHASE	13.94±5.4	11.39±5.44	**<0.001**	0.468	2.55 (1.46, 3.64)
INV_TIME_TO_BRAKING_PHASE	0.18±0.04	0.17±0.05	0.126		0.01 (0, 0.02)
INV_ECCENTRIC_ACCEL_PHASE_DURATION	0.31±0.06	0.31±0.08	0.780		0 (-0.01, 0.02)
INV_ECCENTRIC_DECEL_PHASE_DURATION	0.22±0.06	0.21±0.07	0.322		0.01 (-0.01, 0.02)
INV_BEAKING_CONTRACTION_DURATION_RATIO	40.63±4.49	40.35±6.72	0.669		0.28 (-1, 1.55)
INV_BEAKING_CONCENTRIC_DURATION_RATIO	106.42±18.69	108.74±24.16	0.328		-2.32 (-6.98, 2.34)
INV_MEAN_ECCENTRIC_BRAKING_FORCE	851.17±154.65	811.1±116.74	**0.002**	0.321	40.07 (15.1, 65.04)
INV_MEAN_ECCENTRIC_DECELERATION_FORCE	1038.5±215.71	993.49±179.59	**0.019**	0.241	45 (7.57, 82.44)
INV_FORCE_AT_PEAK_POWER	1270.8±225.57	1327.9±212.25	**0.009**	-0.266	-57.14 (-100.17, -14.1)
INV_CONCENTRIC_IMPULSE_50MS	25.21±8.26	24.7±10.36	0.621		0.51 (-1.5, 2.51)
INV_CONCENTRIC_IMPULSE_100MS	51.47±16.02	51.44±20.81	0.986		0.04 (-3.97, 4.05)
INV_CONCENTRIC_IMPULSE_P1	85.14±18.56	82.59±18.25	0.172		2.56 (-1.11, 6.23)
INV_ECCENTRIC_BRAKING_RFD	2636.1±1369.9	2589.7±1637.2	0.775		46.43 (-272.4, 365.26)
INV_RELATIVE_ECCENTRIC_BRAKING_RFD	34.01±15.95	35.21±21.94	0.574		-1.2 (-5.4, 3)
INV_ECCENTRIC_BRAKING_RFD_100MS	2819.5±1949.2	2648.1±1882.9	0.376		171.48 (-208.31, 551.27)
INV_RELATIVE_ECCENTRIC_BRAKING_RFD_100MS	35.97±23	35.94±25	0.990		0.03 (-4.91, 4.97)
INV_ECCENTRIC_DECEL_RFD	2512.9±1309.3	2651.6±1920.2	0.456		-138.71 (-503.93, 226.5)
INV_RELATIVE_ECCENTRIC_DECEL_RFD	32.61±15.72	36.1±25.83	0.159		-3.49 (-8.36, 1.37)
INV_RELATIVE_PEAK_TAKEOFF_FORCE	18.1±1.63	19.71±2.06	**<0.001**	**-0.807**	-1.6 (-2, -1.21)
INV_PEAK_CONCENTRIC_FORCE	1393.9±257.83	1456.5±249.12	**0.015**	-0.249	-62.6 (-112.85, -12.35)
INV_RELATIVE_PEAK_CONCENTRIC_FORCE	18.1±1.63	19.7±2.06	**<0.001**	**-0.806**	-1.6 (-2, -1.21)
INV_PEAK_ECCENTRIC_FORCE	1248.6±259.93	1195.9±240.02	**0.035**	0.216	52.72 (3.86, 101.58)
INV_RELATIVE_PEAK_ECCENTRIC_FORCE	16.19±1.91	16.2±2.57	0.983		-0.01 (-0.5, 0.49)
INV_RELATIVE_PEAK_LANDING_FORCE	32.48±6.89	40.19±7.11	**<0.001**	**-1.090**	-7.72 (-9.13, -6.3)
INV_MEAN_ECC_CON_POWER_TIME	726.85±243.78	807.66±288.12	**0.005**	-0.288	-80.81 (-137, -24.61)
INV_LOWER_LIMB_STIFFNESS	4838.7±5193.4	6404.1±22940	0.462		-1565.41 (-5740.92, 2610.09)
INV_CONCENTRIC_RPD	9083.4±2887.5	10620±3987.8	**<0.001**	-0.403	-1536.77 (-2299.86, -773.68)
INV_RELATIVE_CONCENTRIC_RPD	118.27±33.56	144.08±51.59	**<0.001**	-0.529	-25.81 (-35.58, -16.04)
INV_CONCENTRIC_RPD_50MS	8575.5±3668.3	8916.7±5356.9	0.511		-341.14 (-1360.43, 678.15)
INV_RELATIVE_CONCENTRIC_RPD_50MS	111.47±43.59	121.31±71.85	0.154		-9.83 (-23.36, 3.69)
INV_CONCENTRIC_RPD_100MS	8863.8±3567.5	9439.3±5186.3	0.253		-575.52 (-1562.78, 411.74)
INV_RELATIVE_CONCENTRIC_RPD_100MS	115.33±42.78	128.41±69.12	**0.049**	-0.201	-13.08 (-26.11, -0.04)
INV_RSI_MODIFIED	15.87±5.64	22.01±6.32	**<0.001**	**-0.988**	-6.13 (-7.38, -4.89)
INV_TOTAL_WORK	517.88±122.53	535.14±119.71	0.160		-17.25 (-41.35, 6.84)
INV_VELOCITY_AT_PEAK_POWER	1.62±0.17	1.78±0.16	**<0.001**	**-1.013**	-0.16 (-0.19, -0.13)
INV_CONCENTRIC_IMPULSE	119.46±24.08	135.09±23.07	**<0.001**	-0.671	-15.63 (-20.29, -10.97)
INV_FORCE_AT_ZERO_VELOCITY	1242.4±258.1	1189.6±240.64	**0.034**	0.216	52.77 (3.88, 101.65)
INV_POSITIVE_IMPULSE	361.75±81.01	381.86±66	**0.004**	-0.291	-20.11 (-33.94, -6.28)
INV_START_OF_INTEGRATION	13.62±5.41	11.08±5.44	**<0.001**	0.468	2.55 (1.46, 3.64)
INV_JUMP_HEIGHT_INCHES	5.25±1.53	7.04±1.3	**<0.001**	**-1.328**	-1.79 (-2.06, -1.52)
INV_JUMP_HEIGHT_INCHES_IMP_MOM	4.99±1.45	6.79±1.39	**<0.001**	**-1.284**	-1.8 (-2.08, -1.52)
INV_TAKEOFF_VELOCITY	1.56±0.24	1.83±0.19	**<0.001**	**-1.355**	-0.27 (-0.31, -0.23)
INV_CONCENTRIC_IMPULSE_P2	34.32±15.93	52.5±19.61	**<0.001**	**-0.957**	-18.19 (-21.99, -14.38)
INV_ECCENTRIC_PEAK_VELOCITY	-0.74±0.22	-0.7±0.24	0.123		-0.04 (-0.08, 0.01)
INV_ECCENTRIC_PEAK_POWER	665.83±276.4	606.12±259.78	**0.026**	0.227	59.71 (7.02, 112.39)
INV_ECCENTRIC_BRAKING_IMPULSE	30.76±11.99	27.06±10.2	**0.001**	0.350	3.7 (1.58, 5.81)
INV_ECCENTRIC_DECEL_IMPULSE	57.33±20.52	51.95±18.99	**0.006**	0.279	5.38 (1.52, 9.25)
INV_ECCENTRIC_UNLOADING_IMPULSE	-57.32±20.51	-51.95±18.99	**0.007**	-0.278	-5.37 (-9.23, -1.5)
INV_POSITIVE_TAKEOFF_IMPULSE	195.98±42.12	200.56±35.77	0.226		-4.58 (-12, 2.84)
INV_CMJ_STIFFNESS	11906±43482	92355±1700000	0.608		-80449.85 (-388054.97, 227155.26)
INV_BODYMASS_RELATIVE_MEAN_TAKEOFF_FORCE	14.56±1.07	15.56±1.31	**<0.001**	-0.784	-1 (-1.25, -0.74)
INV_BODYMASS_RELATIVE_ECCENTRIC_PEAK_POWER	8.58±3.06	8.2±3.3	0.252		0.38 (-0.27, 1.04)
INV_ECC_CON_PEAK_POWER_RATIO	0.32±0.11	0.26±0.11	**<0.001**	0.582	0.06 (0.04, 0.08)
INV_CON_P2_CON_P1_IMPULSE_RATIO	0.44±0.32	0.73±0.62	**<0.001**	-0.506	-0.29 (-0.4, -0.18)

INV_CON_100MS_CON_IMPULSE_RATIO	0.43±0.11	0.39±0.15	**0.001**	0.332	0.05 (0.02, 0.08)
INV_LANDING_IMPULSE	81.81±27.25	71.17±22.44	**<0.001**	0.454	10.64 (5.95, 15.33)
INV_LANDING_RFD_50	25430±9519	35819±13489	**<0.001**	**-0.808**	-10388.88 (-12963.22, -7814.55)
UNINV_START_OF_MOVEMENT	15.52±6.92	11.66±5.35	**<0.001**	0.680	3.86 (2.72, 5)
UNINV_START_OF_MOVEMENT_THRESHOLD	18.39±1	18.33±1.02	0.573		0.06 (-0.15, 0.26)
UNINV_BEGIN_CONCENTRIC_PHASE	16.04±6.92	12.2±5.35	**<0.001**	0.677	3.84 (2.71, 4.98)
UNINV_COUNTERMOVEMENT_DEPTH	-21.55±4.93	-20.65±6.1	0.136		-0.9 (-2.08, 0.28)
UNINV_BODYMASS_RELATIVE_TAKEOFF_POWER	28.94±4.66	31.37±3.99	**<0.001**	-0.589	-2.43 (-3.26, -1.61)
UNINV_FLIGHT_TIME	0.35±0.05	0.38±0.04	**<0.001**	-0.672	-0.03 (-0.03, -0.02)
UNINV_JUMP_HEIGHT	15.56±4.07	17.73±3.28	**<0.001**	-0.632	-2.18 (-2.86, -1.49)
UNINV_JUMP_HEIGHT_RELATIVE_LANDING_RFD	2384.9±1148.9	3273.5±2373.9	**<0.001**	-0.404	-888.63 (-1329.3, -447.95)
UNINV_JUMP_HEIGHT_RELATIVE_PEAK_LANDING_FORCE	171.49±52.23	173.19±39.89	0.695		-1.7 (-10.21, 6.8)
UNINV_IMPULSE_JUMP_HEIGHT	14.76±3.79	17.07±3.54	**<0.001**	-0.645	-2.32 (-3.04, -1.6)
UNINV_JUMP_HEIGHT_IMP_MOM	14.75±3.79	17.07±3.53	**<0.001**	-0.645	-2.32 (-3.03, -1.6)
UNINV_LANDING_RFD	37024±26858	59121±49026	**<0.001**	-0.483	-22097.17 (-31262.69, -12931.65)
UNINV_MEAN_LANDING_ACCELERATION	1.74±0.49	1.88±0.49	**0.006**	-0.285	-0.14 (-0.24, -0.04)
UNINV_MEAN_LANDING_POWER	429.98±127.32	413.65±101.91	0.136		16.32 (-5.13, 37.78)
UNINV_MEAN_LANDING_VELOCITY	-0.15±0.16	-0.1±0.19	**0.002**	-0.312	-0.06 (-0.1, -0.02)
UNINV_MEAN_TAKEOFF_ACCELERATION	5.31±1.2	5.73±1.25	**0.001**	-0.332	-0.41 (-0.66, -0.16)
UNINV_MEAN_TAKEOFF_FORCE	1161.2±188.41	1146.6±168.94	0.409		14.56 (-20.05, 49.17)
UNINV_MEAN_ECCENTRIC_FORCE	756.62±127.47	725.69±97.85	**0.004**	0.297	30.93 (10.1, 51.77)
UNINV_MEAN_ECCENTRIC_POWER	315.02±90.76	279.64±90.97	**<0.001**	0.389	35.39 (17.16, 53.61)
UNINV_MEAN_ECC_CON_RATIO	65.33±5.07	63.65±5.02	**0.001**	0.334	1.68 (0.68, 2.69)
UNINV_MEAN_CONCENTRIC_POWER	1171.9±242.46	1201.3±231.44	0.218		-29.37 (-76.16, 17.42)
UNINV_BODYMASS_RELATIVE_MEAN_CONCENTRIC_POWER	15.31±2.57	16.29±2.5	**<0.001**	-0.389	-0.98 (-1.48, -0.48)
UNINV_BODYMASS_RELATIVE_MEAN_ECCENTRIC_POWER	4.08±0.94	3.78±1.11	**0.007**	0.277	0.3 (0.08, 0.51)
UNINV_MEAN_TAKEOFF_VELOCITY	1.1±0.12	1.13±0.12	**0.010**	-0.262	-0.03 (-0.05, -0.01)
UNINV_PEAK_LANDING_ACCELERATION	23.08±6.16	30.96±7.74	**<0.001**	**-1.053**	-7.88 (-9.37, -6.38)
UNINV_PEAK_LANDING_FORCE	2506.3±501.9	3006.9±666.9	**<0.001**	-0.782	-500.55 (-628.71, -372.39)
UNINV_PEAK_LANDING_POWER	3902.9±1292	4865.4±1555.8	**<0.001**	-0.636	-962.55 (-1265.22, -659.87)
UNINV_PEAK_LANDING_VELOCITY	0.44±0.21	0.47±0.21	0.082		-0.04 (-0.08, 0)
UNINV_PEAK_TAKEOFF_ACCELERATION	8.68±1.76	9.55±1.94	0.000	-0.459	-0.88 (-1.26, -0.5)
UNINV_PEAK_TAKEOFF_FORCE	1421.5±246.24	1431.5±238.59	0.683		-9.99 (-58.09, 38.1)
UNINV_PEAK_TAKEOFF_POWER	2218.6±459.25	2318.2±424.65	**0.024**	-0.231	-99.68 (-186.1, -13.26)
UNINV_PEAK_TAKEOFF_VELOCITY	1.89±0.2	2±0.17	**<0.001**	-0.615	-0.11 (-0.14, -0.07)
UNINV_CONCENTRIC_RFD	1053.3±723.64	1455.6±1039.4	**<0.001**	-0.406	-402.25 (-601.11, -203.39)
UNINV_CONCENTRIC_RFD_100	402.37±1057	741.94±1280.8	**0.008**	-0.273	-339.57 (-588.53, -90.62)
UNINV_CONCENTRIC_RFD_200	-101.5±1306.4	-133.5±1940	0.865		31.97 (-336.58, 400.51)
UNINV_CONCENTRIC_RFD_50	632.69±1293.9	1022.9±1407	**0.006**	-0.281	-390.17 (-668.06, -112.29)
UNINV_CONCENTRIC_RFD_MAX	2515.7±1040.7	2940.2±1455.3	**0.018**	-0.303	-424.52 (-775.36, -73.67)
UNINV_TIME_TO_PEAK_FORCE	0.15±0.08	0.17±0.09	**0.025**	-0.229	-0.02 (-0.04, 0)
UNINV_CONTRACTION_TIME	0.85±0.12	0.87±0.18	0.241		-0.02 (-0.05, 0.01)
UNINV_ECCENTRIC_TIME	0.53±0.09	0.54±0.13	0.229		-0.02 (-0.04, 0.01)
UNINV_START_TO_PEAK_FORCE_TIME	0.67±0.14	0.71±0.19	**0.043**	-0.207	-0.04 (-0.08, 0)
UNINV_START_TO_PEAK_POWER_TIME	0.76±0.12	0.79±0.18	0.192		-0.02 (-0.06, 0.01)
UNINV_WEIGHT_RELATIVE_PEAK_LANDING_FORCE	23.08±6.16	30.96±7.74	**<0.001**	**-1.053**	-7.88 (-9.37, -6.38)
UNINV_WEIGHT_RELATIVE_PEAK_TAKEOFF_FORCE	8.69±1.75	9.56±1.94	**<0.001**	-0.454	-0.87 (-1.25, -0.48)
UNINV_RELATIVE_CONCENTRIC_RFD	13.84±9.14	19.67±13.37	**<0.001**	-0.458	-5.83 (-8.38, -3.27)
UNINV_CONCENTRIC_DURATION	0.33±0.05	0.33±0.07	0.425		-0.01 (-0.02, 0.01)
UNINV_CONCENTRIC_ECCENTRIC_DURATION_RATIO	162.88±7.95	164.18±24	0.563		-1.3 (-5.69, 3.1)
UNINV_ECCENTRIC_CONCENTRIC_DURATION_RATIO	162.66±22.4	167.3±28.27	0.096		-4.65 (-10.12, 0.83)
UNINV_FLIGHT_CONTRACTION_TIME_RATIO	0.43±0.09	0.46±0.1	**0.004**	-0.292	-0.03 (-0.05, -0.01)
UNINV_FLIGHT_ECCENTRIC_TIME_RATIO	0.7±0.16	0.76±0.24	**0.010**	-0.266	-0.06 (-0.1, -0.01)
UNINV_BEGIN_BRAKING_PHASE	15.69±6.92	11.83±5.35	**<0.001**	0.680	3.86 (2.72, 4.99)
UNINV_MIN_ECCENTRIC_FORCE	375.67±142.2	394.07±148.88	0.223		-18.4 (-47.99, 11.19)
UNINV_BRAKING_PHASE_DURATION	0.35±0.07	0.37±0.11	0.206		-0.01 (-0.04, 0.01)

UNINV_BEGIN_ECC_DECEL_PHASE	15.83±6.92	11.98±5.34	**<0.001**	0.679	3.85 (2.72, 4.99)
UNINV_TIME_TO_BRAKING_PHASE	0.17±0.04	0.17±0.05	0.806		0 (-0.01, 0.01)
UNINV_ECCENTRIC_ACCEL_PHASE_DURATION	0.32±0.06	0.32±0.07	0.460		-0.01 (-0.02, 0.01)
UNINV_ECCENTRIC_DECEL_PHASE_DURATION	0.21±0.05	0.22±0.08	0.196		-0.01 (-0.02, 0)
UNINV_BEAKING_CONTRACTION_DURATION_RATIO	41.12±3.57	41.04±5.82	0.887		0.08 (-1.02, 1.18)
UNINV_BEAKING_CONCENTRIC_DURATION_RATIO	108.29±15.61	111.05±23.97	0.234		-2.76 (-7.3, 1.78)
UNINV_MEAN_ECCENTRIC_BRAKING_FORCE	851.31±148.59	813.95±116.56	**0.003**	0.303	37.36 (12.69, 62.03)
UNINV_MEAN_ECCENTRIC_DECELERATION_FORCE	1061.4±196.56	998.31±172.55	**0.001**	0.355	63.05 (27.53, 98.56)
UNINV_FORCE_AT_PEAK_POWER	1303±221.23	1300.7±203.32	0.914		2.27 (-39.16, 43.7)
UNINV_CONCENTRIC_IMPULSE_50MS	26.76±7.79	25.44±9.8	0.173		1.32 (-0.58, 3.21)
UNINV_CONCENTRIC_IMPULSE_100MS	54.34±15.91	52.62±19.46	0.372		1.72 (-2.06, 5.5)
UNINV_CONCENTRIC_IMPULSE_P1	86.96±17.07	84.41±16.79	0.140		2.54 (-0.83, 5.92)
UNINV_ECCENTRIC_BRAKING_RFD	2775.8±1230.4	2615.5±1539.3	0.291		160.29 (-137.67, 458.25)
UNINV_RELATIVE_ECCENTRIC_BRAKING_RFD	36.23±15.41	35.65±20.66	0.771		0.59 (-3.38, 4.55)
UNINV_ECCENTRIC_BRAKING_RFD_100MS	2811.3±1684.4	2661.6±1882.5	0.427		149.7 (-220.49, 519.89)
UNINV_RELATIVE_ECCENTRIC_BRAKING_RFD_100MS	36.23±20.77	36.12±24.77	0.965		0.11 (-4.72, 4.93)
UNINV_ECCENTRIC_DECEL_RFD	2721.3±1248.5	2665.5±1711	0.738		55.81 (-271.88, 383.5)
UNINV_RELATIVE_ECCENTRIC_DECEL_RFD	35.83±16.26	36.41±23.27	0.800		-0.57 (-5.01, 3.86)
UNINV_RELATIVE_PEAK_TAKEOFF_FORCE	18.5±1.75	19.37±1.94	**<0.001**	-0.454	-0.87 (-1.25, -0.48)
UNINV_PEAK_CONCENTRIC_FORCE	1420.1±245.85	1431±238.63	0.656		-10.93 (-59.02, 37.16)
UNINV_RELATIVE_PEAK_CONCENTRIC_FORCE	18.48±1.76	19.36±1.94	**<0.001**	-0.459	-0.88 (-1.26, -0.5)
UNINV_PEAK_ECCENTRIC_FORCE	1277.8±232.96	1211.6±230.76	**0.005**	0.286	66.21 (19.89, 112.53)
UNINV_RELATIVE_PEAK_ECCENTRIC_FORCE	16.63±1.82	16.42±2.43	0.369		0.21 (-0.25, 0.68)
UNINV_RELATIVE_PEAK_LANDING_FORCE	32.89±6.16	40.77±7.74	**<0.001**	**-1.053**	-7.88 (-9.37, -6.38)
UNINV_MEAN_ECC_CON_POWER_TIME	785.21±237.07	786.85±263.09	0.950		-1.64 (-53.44, 50.15)
UNINV_LOWER_LIMB_STIFFNESS	4374.1±1519.7	5237±11872	0.431		-862.92 (-3014.51, 1288.67)
UNINV_CONCENTRIC_RPD	9824.8±3141.6	10359±3664.6	0.143		-534.43 (-1250.5, 181.65)
UNINV_RELATIVE_CONCENTRIC_RPD	128.89±40.14	140.61±47.11	**0.013**	-0.255	-11.72 (-20.92, -2.53)
UNINV_CONCENTRIC_RPD_50MS	9333.1±3806.8	9183±5010.8	0.760		150.11 (-813.87, 1114.09)
UNINV_RELATIVE_CONCENTRIC_RPD_50MS	122.77±49.39	125.1±67.15	0.722		-2.34 (-15.21, 10.54)
UNINV_CONCENTRIC_RPD_100MS	9563±3948.4	9587.6±4774.7	0.959		-24.57 (-952.91, 903.76)
UNINV_RELATIVE_CONCENTRIC_RPD_100MS	125.81±51.47	130.55±63.75	0.451		-4.74 (-17.1, 7.61)
UNINV_RSI_MODIFIED	18.89±6.21	21.43±5.77	**<0.001**	-0.432	-2.53 (-3.71, -1.36)
UNINV_TOTAL_WORK	541.83±120.83	540.65±119	0.923		1.18 (-22.74, 25.09)
UNINV_VELOCITY_AT_PEAK_POWER	1.7±0.17	1.78±0.16	**<0.001**	-0.516	-0.08 (-0.11, -0.05)
UNINV_CONCENTRIC_IMPULSE	129.28±24.19	134.32±22.39	**0.030**	-0.221	-5.04 (-9.59, -0.48)
UNINV_FORCE_AT_ZERO_VELOCITY	1272±231.08	1204.6±231.01	**0.004**	0.291	67.33 (21.03, 113.62)
UNINV_POSITIVE_IMPULSE	384.96±77.3	381.78±64.32	0.641		3.18 (-10.23, 16.59)
UNINV_START_OF_INTEGRATION	15.52±6.92	11.66±5.35	**<0.001**	0.680	3.86 (2.72, 5)
UNINV_JUMP_HEIGHT_INCHES	6.12±1.6	6.98±1.29	**<0.001**	-0.632	-0.86 (-1.13, -0.59)
UNINV_JUMP_HEIGHT_INCHES_IMP_MOM	5.81±1.49	6.72±1.39	**<0.001**	-0.645	-0.91 (-1.19, -0.63)
UNINV_TAKEOFF_VELOCITY	1.69±0.22	1.82±0.19	**<0.001**	-0.670	-0.13 (-0.17, -0.09)
UNINV_CONCENTRIC_IMPULSE_P2	42.32±14.29	49.9±17.75	**<0.001**	-0.441	-7.58 (-11.02, -4.14)
UNINV_ECCENTRIC_PEAK_VELOCITY	-0.79±0.19	-0.73±0.22	**0.007**	-0.275	-0.06 (-0.1, -0.02)
UNINV_ECCENTRIC_PEAK_POWER	706.89±243.95	625.33±251.74	**0.001**	0.325	81.56 (31.4, 131.72)
UNINV_ECCENTRIC_BRAKING_IMPULSE	31.1±9.97	28.3±11	**0.011**	0.258	2.8 (0.63, 4.97)
UNINV_ECCENTRIC_DECEL_IMPULSE	60.67±18.11	53.64±18.41	**<0.001**	0.382	7.03 (3.35, 10.71)
UNINV_ECCENTRIC_UNLOADING_IMPULSE	-60.66±18.1	-53.64±18.41	**<0.001**	-0.382	-7.02 (-10.7, -3.35)
UNINV_POSITIVE_TAKEOFF_IMPULSE	206.26±40.56	201.43±34.99	0.190		4.83 (-2.4, 12.06)
UNINV_CMJ_STIFFNESS	7090.3±2513.6	38779±575858	0.550		-31688.42 (-135857.88, 72481.04)
UNINV_BODYMASS_RELATIVE_MEAN_TAKEOFF_FORCE	15.12±1.2	15.53±1.25	**0.001**	-0.332	-0.41 (-0.66, -0.16)
UNINV_BODYMASS_RELATIVE_ECCENTRIC_PEAK_POWER	9.16±2.77	8.46±3.16	**0.027**	0.226	0.7 (0.08, 1.32)
UNINV_ECC_CON_PEAK_POWER_RATIO	0.32±0.09	0.28±0.11	**<0.001**	0.434	0.05 (0.02, 0.07)
UNINV_CON_P2_CON_P1_IMPULSE_RATIO	0.5±0.18	0.65±0.37	**<0.001**	-0.428	-0.15 (-0.22, -0.08)
UNINV_CON_100MS_CON_IMPULSE_RATIO	0.42±0.1	0.4±0.15	0.068		0.03 (0, 0.05)
UNINV_LANDING_IMPULSE	81.77±27.13	72.74±25.01	**0.001**	0.355	9.03 (3.94, 14.13)
UNINV_LANDING_RFD_50	26639±9187.6	37071±14264	**<0.001**	-0.774	-10432.52 (-13131.6, -7733.43)
LSI_START_OF_MOVEMENT	99.73±54.02	105.13±54.85	0.334		-5.39 (-16.35, 5.57)

LSI_START_OF_MOVEMENT_THRESHOLD	100.22±6.39	101.37±26.24	0.636		-1.15 (-5.93, 3.63)
LSI_BEGIN_CONCENTRIC_PHASE	99.42±51.31	103.95±49.38	0.373		-4.53 (-14.49, 5.44)
LSI_COUNTERMOVEMENT_DEPTH	96.73±17.88	99.57±32.08	0.354		-2.84 (-8.84, 3.17)
LSI_BODYMASS_RELATIVE_TAKEOFF_POWER	93.03±6.97	102.53±9.84	**<0.001**	**-1.011**	-9.49 (-11.37, -7.61)
LSI_FLIGHT_TIME	92.29±5.96	100.65±6.77	**<0.001**	**-1.259**	-8.35 (-9.68, -7.03)
LSI_JUMP_HEIGHT	85.53±10.86	101.73±13.61	**<0.001**	**-1.231**	-16.2 (-18.84, -13.57)
LSI_JUMP_HEIGHT_RELATIVE_LANDING_RFD	114.91±28.68	101.12±31.06	**<0.001**	0.450	13.79 (7.65, 19.93)
LSI_JUMP_HEIGHT_RELATIVE_PEAK_LANDING_FORCE	117.46±19.8	99.08±14.66	**<0.001**	**1.167**	18.38 (15.23, 21.54)
LSI_IMPULSE_JUMP_HEIGHT	85.71±11.18	102.37±16.55	**<0.001**	**-1.060**	-16.65 (-19.8, -13.51)
LSI_JUMP_HEIGHT_IMP_MOM	85.67±11.17	102.39±16.5	**<0.001**	**-1.067**	-16.72 (-19.86, -13.58)
LSI_LANDING_RFD	97.78±26.47	103.1±36	0.131		-5.32 (-12.22, 1.58)
LSI_MEAN_LANDING_ACCELERATION	82.36±70.76	106.62±78.13	**0.002**	-0.315	-24.27 (-39.71, -8.82)
LSI_MEAN_LANDING_POWER	95.22±18.7	102.24±22.11	**0.001**	-0.326	-7.02 (-11.33, -2.71)
LSI_MEAN_LANDING_VELOCITY	119.68±364.89	67.49±1206.6	0.642		52.19 (-168.33, 272.72)
LSI_MEAN_TAKEOFF_ACCELERATION	90.08±11.29	101.25±14.77	**<0.001**	-0.786	-11.17 (-14.01, -8.33)
LSI_MEAN_TAKEOFF_FORCE	96.41±4.06	100.26±5.12	**<0.001**	-0.776	-3.84 (-4.83, -2.85)
LSI_MEAN_ECCENTRIC_FORCE	99.99±0.07	100.07±0.79	0.280		-0.08 (-0.22, 0.06)
LSI_MEAN_ECCENTRIC_POWER	94.66±17.56	99.09±27.81	0.098		-4.43 (-9.69, 0.82)
LSI_MEAN_ECC_CON_RATIO	103.9±4.39	100.1±5.29	**<0.001**	0.739	3.8 (2.77, 4.83)
LSI_MEAN_CONCENTRIC_POWER	92.6±7.9	100.1±11.25	**<0.001**	-0.700	-7.5 (-9.65, -5.36)
LSI_BODYMASS_RELATIVE_MEAN_CONCENTRIC_POWER	92.6±7.9	100.1±11.29	**<0.001**	-0.697	-7.5 (-9.65, -5.35)
LSI_BODYMASS_RELATIVE_MEAN_ECCENTRIC_POWER	94.66±17.56	99.08±27.8	0.099		-4.41 (-9.67, 0.84)
LSI_MEAN_TAKEOFF_VELOCITY	96.36±6.35	99.29±8.61	**0.001**	-0.355	-2.93 (-4.58, -1.28)
LSI_PEAK_LANDING_ACCELERATION	99.03±18.43	99.98±17.21	0.596		-0.94 (-4.44, 2.55)
LSI_PEAK_LANDING_FORCE	99.11±12.36	99.64±12.72	0.680		-0.53 (-3.07, 2)
LSI_PEAK_LANDING_POWER	92.85±16.82	102.23±20.57	**<0.001**	-0.470	-9.38 (-13.38, -5.39)
LSI_PEAK_LANDING_VELOCITY	105.18±120.52	103.76±116.4	0.906		1.42 (-22.06, 24.9)
LSI_PEAK_TAKEOFF_ACCELERATION	96.44±12.79	104.34±13.81	**<0.001**	-0.579	-7.9 (-10.63, -5.17)
LSI_PEAK_TAKEOFF_FORCE	98.05±5.83	101.93±6.62	**<0.001**	-0.596	-3.87 (-5.17, -2.57)
LSI_PEAK_TAKEOFF_POWER	93.03±6.97	102.52±9.73	**<0.001**	**-1.021**	-9.49 (-11.35, -7.63)
LSI_PEAK_TAKEOFF_VELOCITY	95.36±4.49	100.72±6.61	**<0.001**	**-0.853**	-5.35 (-6.61, -4.1)
LSI_CONCENTRIC_RFD	148.5±201.44	145.46±231.58	0.896		3.04 (-42.47, 48.55)
LSI_CONCENTRIC_RFD_100	157±1133.2	114.39±1197.6	0.725		42.6 (-195.04, 280.25)
LSI_CONCENTRIC_RFD_200	546.47±8952.7	300.2±4503.8	0.667		246.27 (-876.53, 1369.06)
LSI_CONCENTRIC_RFD_50	201.45±1058	139.16±660.14	0.416		62.29 (-87.98, 212.55)
LSI_CONCENTRIC_RFD_MAX	105.49±46.08	125.15±57.75	**0.011**	-0.349	-19.66 (-34.88, -4.44)
LSI_TIME_TO_PEAK_FORCE	167.42±405.63	241.2±1396.3	0.572		-73.77 (-329.82, 182.28)
LSI_CONTRACTION_TIME	102.77±11.29	99.82±14.77	**0.042**	0.208	2.95 (0.11, 5.79)
LSI_ECCENTRIC_TIME	102.39±14.07	99.64±22.64	0.207		2.75 (-1.52, 7.02)
LSI_START_TO_PEAK_FORCE_TIME	103.15±18.9	101.82±20.36	0.518		1.33 (-2.7, 5.35)
LSI_START_TO_PEAK_POWER_TIME	102.08±12.54	99.93±16.42	0.181		2.16 (-1.01, 5.32)
LSI_WEIGHT_RELATIVE_PEAK_LANDING_FORCE	99.03±18.43	99.98±17.21	0.596		-0.94 (-4.44, 2.55)
LSI_WEIGHT_RELATIVE_PEAK_TAKEOFF_FORCE	96.3±12.71	104.33±13.76	**<0.001**	-0.591	-8.03 (-10.75, -5.31)
LSI_RELATIVE_CONCENTRIC_RFD	148.5±201.39	145.45±231.55	0.895		3.05 (-42.46, 48.55)
LSI_CONCENTRIC_DURATION	103.9±11.91	101.57±15.25	0.121		2.33 (-0.61, 5.27)
LSI_CONCENTRIC_ECCENTRIC_DURATION_RATIO	101.64±11.78	101.29±17.26	0.835		0.35 (-2.95, 3.65)
LSI_ECCENTRIC_CONCENTRIC_DURATION_RATIO	99.37±12.77	101.59±16.61	0.175		-2.22 (-5.44, 0.99)
LSI_FLIGHT_CONTRACTION_TIME_RATIO	91.15±12.82	102.48±16.63	**<0.001**	-0.710	-11.33 (-14.55, -8.11)
LSI_FLIGHT_ECCENTRIC_TIME_RATIO	93.64±27.62	105.11±32.33	**<0.001**	-0.364	-11.47 (-17.82, -5.12)
LSI_BEGIN_BRAKING_PHASE	99.63±53.1	104.7±52.72	0.347		-5.07 (-15.65, 5.51)
LSI_MIN_ECCENTRIC_FORCE	114.04±40.1	106.85±38.67	0.071		7.19 (-0.61, 15)
LSI_BRAKING_PHASE_DURATION	102.42±19.08	100.71±25.86	0.498		1.71 (-3.25, 6.67)
LSI_BEGIN_ECC_DECEL_PHASE	99.5±52.37	104.35±51.08	0.354		-4.86 (-15.14, 5.43)
LSI_TIME_TO_BRAKING_PHASE	104.91±24.77	101.89±35.99	0.388		3.02 (-3.84, 9.87)
LSI_ECCENTRIC_ACCEL_PHASE_DURATION	101.13±16.79	99.61±22.9	0.496		1.52 (-2.87, 5.91)
LSI_ECCENTRIC_DECEL_PHASE_DURATION	106.39±25.18	101.66±31.14	0.124		4.73 (-1.3, 10.77)
LSI_BEAKING_CONTRACTION_DURATION_RATIO	99.21±11.37	99.54±18.13	0.850		-0.33 (-3.75, 3.09)
LSI_BEAKING_CONCENTRIC_DURATION_RATIO	99.04±15.48	100.28±22.81	0.573		-1.24 (-5.58, 3.09)
LSI_MEAN_ECCENTRIC_BRAKING_FORCE	99.93±3.8	99.72±4.08	0.614		0.21 (-0.6, 1.01)

LSI_MEAN_ECCENTRIC_DECELERATION_FORCE	97.71±7.24	99.69±7.76	**0.012**	-0.257	-1.97 (-3.51, -0.44)
LSI_FORCE_AT_PEAK_POWER	97.52±5.1	102.21±5.93	**<0.001**	**-0.810**	-4.69 (-5.85, -3.53)
LSI_CONCENTRIC_IMPULSE_50MS	95.67±22.96	100.77±40.21	0.184		-5.1 (-12.64, 2.43)
LSI_CONCENTRIC_IMPULSE_100MS	96.25±21.69	101.07±38.3	0.187		-4.82 (-12, 2.35)
LSI_CONCENTRIC_IMPULSE_P1	98±10.12	98.39±14.3	0.781		-0.39 (-3.12, 2.34)
LSI_ECCENTRIC_BRAKING_RFD	97.13±33.55	107.07±55.12	0.061		-9.94 (-20.32, 0.44)
LSI_RELATIVE_ECCENTRIC_BRAKING_RFD	97.14±33.54	107.07±55.17	0.061		-9.94 (-20.33, 0.46)
LSI_ECCENTRIC_BRAKING_RFD_100MS	111.45±69.99	118.98±137.99	0.565		-7.52 (-33.2, 18.15)
LSI_RELATIVE_ECCENTRIC_BRAKING_RFD_100MS	111.45±69.98	118.99±138.01	0.564		-7.54 (-33.22, 18.14)
LSI_ECCENTRIC_DECEL_RFD	97.25±43.35	110.72±89.38	0.111		-13.47 (-30.06, 3.13)
LSI_RELATIVE_ECCENTRIC_DECEL_RFD	97.25±43.35	110.71±89.42	0.112		-13.46 (-30.06, 3.14)
LSI_RELATIVE_PEAK_TAKEOFF_FORCE	98.06±5.83	101.92±6.64	**<0.001**	-0.594	-3.86 (-5.17, -2.56)
LSI_PEAK_CONCENTRIC_FORCE	98.11±5.87	101.93±6.65	**<0.001**	-0.586	-3.82 (-5.12, -2.51)
LSI_RELATIVE_PEAK_CONCENTRIC_FORCE	98.12±5.86	101.93±6.67	**<0.001**	-0.583	-3.81 (-5.12, -2.5)
LSI_PEAK_ECCENTRIC_FORCE	97.68±9.26	98.99±9.88	0.187		-1.31 (-3.27, 0.64)
LSI_RELATIVE_PEAK_ECCENTRIC_FORCE	97.68±9.25	98.98±9.85	0.190		-1.3 (-3.26, 0.65)
LSI_RELATIVE_PEAK_LANDING_FORCE	99.11±12.36	99.64±12.75	0.683		-0.53 (-3.07, 2.01)
LSI_MEAN_ECC_CON_POWER_TIME	93.58±21.06	107.28±40.29	**<0.001**	-0.365	-13.7 (-21.21, -6.19)
LSI_LOWER_LIMB_STIFFNESS	115.41±145.89	132.79±282.85	0.518		-17.38 (-70.21, 35.45)
LSI_CONCENTRIC_RPD	93.89±18.72	104±21.8	**<0.001**	-0.475	-10.11 (-14.38, -5.85)
LSI_RELATIVE_CONCENTRIC_RPD	93.9±18.72	104±21.81	**<0.001**	-0.475	-10.11 (-14.37, -5.84)
LSI_CONCENTRIC_RPD_50MS	95.63±31.54	103.4±56.38	0.149		-7.77 (-18.32, 2.78)
LSI_RELATIVE_CONCENTRIC_RPD_50MS	95.64±31.53	103.39±56.36	0.150		-7.75 (-18.3, 2.8)
LSI_CONCENTRIC_RPD_100MS	96.43±29.89	104.04±52.36	0.129		-7.61 (-17.42, 2.21)
LSI_RELATIVE_CONCENTRIC_RPD_100MS	96.44±29.89	104.02±52.34	0.129		-7.59 (-17.4, 2.23)
LSI_RSI_MODIFIED	84.46±14.92	104.96±25.13	**<0.001**	**-0.869**	-20.51 (-25.23, -15.78)
LSI_TOTAL_WORK	95.69±8.65	99.47±10.35	**<0.001**	-0.376	-3.79 (-5.8, -1.77)
LSI_VELOCITY_AT_PEAK_POWER	95.38±4.44	100.25±6.73	**<0.001**	-0.764	-4.87 (-6.15, -3.6)
LSI_CONCENTRIC_IMPULSE	92.33±6.09	100.84±7.99	**<0.001**	**-1.107**	-8.51 (-10.04, -6.97)
LSI_FORCE_AT_ZERO_VELOCITY	97.65±9.39	99.07±10.26	0.168		-1.42 (-3.45, 0.6)
LSI_POSITIVE_IMPULSE	93.79±7.15	100.22±7.43	**<0.001**	**-0.871**	-6.43 (-7.91, -4.96)
LSI_START_OF_INTEGRATION	99.73±54.02	105.13±54.85	0.334		-5.39 (-16.35, 5.57)
LSI_JUMP_HEIGHT_INCHES	85.53±10.86	101.73±13.61	**<0.001**	**-1.231**	-16.2 (-18.84, -13.57)
LSI_JUMP_HEIGHT_INCHES_IMP_MOM	85.67±11.17	102.39±16.5	**<0.001**	**-1.067**	-16.72 (-19.86, -13.58)
LSI_TAKEOFF_VELOCITY	92.35±6.09	100.84±8.09	**<0.001**	**-1.093**	-8.49 (-10.05, -6.94)
LSI_CONCENTRIC_IMPULSE_P2	80.44±28.73	107.83±46.43	**<0.001**	-0.626	-27.38 (-36.14, -18.63)
LSI_ECCENTRIC_PEAK_VELOCITY	94.14±17.8	99.15±27.88	0.063		-5.01 (-10.28, 0.27)
LSI_ECCENTRIC_PEAK_POWER	94±21.55	99.99±31.76	0.052		-5.99 (-12.02, 0.05)
LSI_ECCENTRIC_BRAKING_IMPULSE	99.49±25.78	101.59±38.38	0.571		-2.1 (-9.39, 5.19)
LSI_ECCENTRIC_DECEL_IMPULSE	94.16±17.83	99.16±27.88	0.063		-5 (-10.27, 0.27)
LSI_ECCENTRIC_UNLOADING_IMPULSE	94.13±17.8	99.16±27.9	0.062		-5.02 (-10.3, 0.25)
LSI_POSITIVE_TAKEOFF_IMPULSE	94.85±5.76	99.77±7.54	**<0.001**	-0.679	-4.92 (-6.37, -3.47)
LSI_CMJ_STIFFNESS	157.31±480.36	210.29±1318.2	0.668		-52.98 (-295.34, 189.38)
LSI_BODYMASS_RELATIVE_MEAN_TAKEOFF_FORCE	96.42±4.06	100.25±5.13	**<0.001**	-0.774	-3.83 (-4.82, -2.84)
LSI_BODYMASS_RELATIVE_ECCENTRIC_PEAK_POWER	94.01±21.55	99.98±31.75	0.053		-5.97 (-12.01, 0.07)
LSI_ECC_CON_PEAK_POWER_RATIO	101.87±25.29	98.97±33.83	0.380		2.9 (-3.59, 9.4)
LSI_CON_P2_CON_P1_IMPULSE_RATIO	87.63±54.85	118±82.21	**<0.001**	-0.389	-30.36 (-45.97, -14.76)
LSI_CON_100MS_CON_IMPULSE_RATIO	104.67±24.32	100.78±38.13	0.289		3.9 (-3.31, 11.1)
LSI_LANDING_IMPULSE	102.67±25.45	101.87±26.07	0.763		0.8 (-4.4, 6)
LSI_LANDING_RFD_50	98.16±26.87	100.79±29	0.369		-2.63 (-8.36, 3.11)

Drop jump

	ACLR n=65	Controls n=100	p value	d	Mean difference (95% CIs)
BEGIN_CONCENTRIC_PHASE	17.36±6.11	16.77±7.13	0.584		0.59 (-1.53, 2.71)
COUNTERMOVEMENT_DEPTH	-23.89±6.67	-21.39±7.27	**0.027**	-0.353	-2.5 (-4.71, -0.29)
BODYMASS_RELATIVE_TAKEOFF_POWER	120.17±22.3	139.79±38.14	**<0.001**	-0.595	-19.62 (-29.95, -9.29)
CONTACT_TIME	0.36±0.1	0.32±0.11	**0.015**	0.390	0.04 (0.01, 0.08)
FLIGHT_TIME	0.5±0.06	0.53±0.04	**0.001**	-0.534	-0.03 (-0.04, -0.01)
JUMP_HEIGHT	31.55±7.33	34.53±4.87	**0.002**	-0.497	-2.97 (-4.85, -1.1)
JUMP_HEIGHT_RELATIVE_LANDING_RFD	1809.4±1421.6	2845.7±1758.4	**<0.001**	-0.631	-1036.28 (-1550.5, -522.05)
JUMP_HEIGHT_RELATIVE_PEAK_LANDING_FORCE	116.46±44.74	146.73±43.34	**<0.001**	-0.686	-30.27 (-44.08, -16.46)
IMPULSE_JUMP_HEIGHT	31.6±7.34	34.62±4.88	**0.002**	-0.505	-3.02 (-4.9, -1.15)
JUMP_HEIGHT_IMP_MOM	31.6±7.33	34.66±4.89	**0.002**	-0.510	-3.06 (-4.94, -1.18)
LANDING_RFD	56320±52391	97220±61545	**<0.001**	-0.700	-40900.02 (-59185.86, -22614.19)
JUMP_HEIGHT_INCHES	12.42±2.89	13.59±1.92	**0.002**	-0.495	-1.17 (-1.91, -0.43)
JUMP_HEIGHT_INCHES_IMP_MOM	12.44±2.89	13.64±1.93	**0.002**	-0.508	-1.2 (-1.94, -0.46)
MEAN_LANDING_ACCELERATION	2.16±1.01	2.08±1.42	0.672		0.09 (-0.32, 0.49)
MEAN_LANDING_POWER	1911.9±377.92	1789.8±389.49	**0.048**	0.316	122.12 (1, 243.24)
MEAN_LANDING_VELOCITY	-0.2±0.48	-0.37±0.97	0.195		0.17 (-0.09, 0.43)
MEAN_TAKEOFF_ACCELERATION	13.53±3.35	17.09±5.32	**<0.001**	-0.762	-3.56 (-5.02, -2.1)
MEAN_TAKEOFF_FORCE	1835.7±346.75	2090.6±530.21	**0.001**	-0.543	-254.91 (-401.79, -108.03)
MEAN_ECCENTRIC_FORCE	1988.4±451.4	2166.5±685.31	0.066		-178.14 (-368.28, 12)
MEAN_ECC_CON_RATIO	108.1±10.3	102.65±12.06	**0.003**	0.476	5.45 (1.86, 9.04)
MEAN_CONCENTRIC_POWER	6839.7±1325.1	7815±2237.3	**0.002**	-0.503	-975.33 (-1582.91, -367.75)
BODYMASS_RELATIVE_MEAN_CONCENTRIC_POWER	87.22±14.44	100.46±23.15	**<0.001**	-0.653	-13.24 (-19.59, -6.89)
MEAN_TAKEOFF_VELOCITY	1.69±0.15	1.77±0.13	**<0.001**	-0.608	-0.09 (-0.13, -0.04)
PEAK_LANDING_ACCELERATION	34.34±13.53	54.49±17.26	**<0.001**	**-1.261**	-20.15 (-25.15, -15.14)
PEAK_LANDING_FORCE	3447.2±1085.9	4957.3±1409	**<0.001**	**-1.164**	-1510.09 (-1916.5, -1103.67)
PEAK_LANDING_POWER	4072.8±1156.3	5157.2±1886.4	**<0.001**	-0.659	-1084.45 (-1600.09, -568.82)
PEAK_LANDING_VELOCITY	0.72±0.42	0.71±0.28	0.896		0.01 (-0.1, 0.11)
PEAK_TAKEOFF_ACCELERATION	24.22±7.72	31.49±13.37	**<0.001**	-0.629	-7.26 (-10.88, -3.65)
PEAK_TAKEOFF_POWER	9430±2000.6	10895±3538.9	**0.003**	-0.481	-1465.32 (-2418.43, -512.2)
PEAK_TAKEOFF_VELOCITY	2.62±0.28	2.72±0.18	**0.005**	-0.449	-0.1 (-0.17, -0.03)
RSI	93.68±28.9	123.55±43.55	**<0.001**	-0.773	-29.87 (-41.97, -17.77)
REACTIVE_STRENGTH_INDEX	1.51±0.39	1.9±0.64	**<0.001**	-0.695	-0.39 (-0.56, -0.21)
START_TO_PEAK_POWER_TIME	0.27±0.11	0.24±0.11	0.050		0.04 (0, 0.07)
WEIGHT_RELATIVE_PEAK_LANDING_FORCE	34.34±13.53	54.49±17.26	**<0.001**	**-1.261**	-20.15 (-25.15, -15.14)
PEAK_DROP_FORCE	3124±796.45	3621.4±1286.6	**0.006**	-0.442	-497.38 (-849.76, -145)
CONTACT_VELOCITY	-2.31±0.14	-2.25±0.28	0.148		-0.05 (-0.13, 0.02)
DROP_HEIGHT	27.52±3.22	26.4±6.03	0.172		1.12 (-0.49, 2.73)
EFFECTIVE_DROP	27.52±3.22	26.4±6.03	0.172		1.12 (-0.49, 2.73)
DROP_LANDING	17.2±6.1	16.62±7.13	0.594		0.57 (-1.55, 2.7)
TAKEOFF_VELOCITY	2.47±0.3	2.6±0.18	**0.001**	-0.546	-0.13 (-0.2, -0.06)
PEAK_IMPACT_FORCE	2789.2±818.79	3208.4±1301.9	**0.022**	-0.367	-419.21 (-776.91, -61.51)
CONTACT_TROUGH	2065.2±620.65	2546.2±1230.1	**0.004**	-0.463	-481.06 (-806.55, -155.58)
PEAK_DRIVEOFF_FORCE	2731.5±721.16	3254.6±1212.1	**0.002**	-0.497	-523.13 (-852.58, -193.68)
PASSIVE_STIFFNESS	13083±6677.1	18429±13063	**0.003**	-0.483	-5346.05 (-8808.75, -1883.35)
ACTIVE_STIFFNESS	13018±6525.7	18826±12390	**0.001**	-0.551	-5808.05 (-9107.09, -2509)
PASSIVE_STIFFNESS_INDEX	4.66±2.29	6.43±4.88	**0.007**	-0.432	-1.76 (-3.04, -0.49)
ACTIVE_STIFFNESS_INDEX	4.59±2.23	6.54±4.56	**0.002**	-0.506	-1.94 (-3.14, -0.74)
CONCENTRIC_IMPULSE	194.5±34.82	201.2±31.39	0.201		-6.71 (-17.02, 3.61)
FORCE_AT_ZERO_VELOCITY	2599.6±689.4	3147.7±1223.7	**0.001**	-0.521	-548.1 (-877.48, -218.73)
POSITIVE_IMPULSE	647.1±111.43	646.08±100.59	0.952		1.01 (-32.01, 34.04)
ECCENTRIC_IMPULSE	181.89±27.13	173.92±31.87	0.098		7.97 (-1.5, 17.44)
POSITIVE_TAKEOFF_IMPULSE	394±62.39	391.41±58.99	0.788		2.58 (-16.4, 21.57)
DROP_LANDING_RFD	39944±19061	53060±32826	**0.004**	-0.462	-13116.12 (-21998.6, -4233.63)

INV_LANDING_RFD	29234±27095	52854±34019	**<0.001**	-0.747	-23619.3 (-33523.89, -13714.7)
INV_MEAN_TAKEOFF_FORCE	861.06±169.54	1042±282.15	**<0.001**	-0.738	-180.97 (-257.8, -104.14)
INV_MEAN_ECCENTRIC_FORCE	948.55±224.76	1067.8±406.63	**0.032**	-0.342	-119.27 (-228.38, -10.17)
INV_MEAN_ECC_CON_RATIO	110.58±14.72	100.75±18.29	**<0.001**	0.577	9.84 (4.5, 15.18)
INV_PEAK_LANDING_FORCE	1745±562.22	2626±791.28	**<0.001**	**-1.235**	-880.94 (-1104.38, -657.5)
INV_PEAK_DROP_FORCE	1561.6±379.78	1897.5±694.43	**<0.001**	-0.566	-335.89 (-521.89, -149.89)
INV_PEAK_IMPACT_FORCE	1400.3±398.81	1689.7±726.75	**0.004**	-0.465	-289.48 (-484.24, -94.71)
INV_PEAK_DRIVEOFF_FORCE	1314.1±350.67	1622.8±625.1	**<0.001**	-0.575	-308.7 (-476.83, -140.57)
INV_PASSIVE_STIFFNESS	12604±6737	17868±12974	**0.003**	-0.478	-5264.36 (-8711.5, -1817.22)
INV_ACTIVE_STIFFNESS	12890±6524.2	18702±12405	**0.001**	-0.551	-5811.72 (-9114, -2509.43)
INV_CONCENTRIC_IMPULSE	163.33±41.48	163.4±30.28	0.991		-0.07 (-11.11, 10.98)
INV_FORCE_AT_ZERO_VELOCITY	1238.9±326.57	1548.5±634.55	**<0.001**	-0.576	-309.6 (-477.98, -141.22)
INV_POSITIVE_IMPULSE	572.4±152.27	516.76±104.43	**0.006**	0.442	55.65 (16.19, 95.1)
INV_ECCENTRIC_IMPULSE	148.12±34.2	138.82±33.95	0.088		9.3 (-1.41, 20.01)
INV_POSITIVE_TAKEOFF_IMPULSE	305.63±71.97	296.67±58.57	0.382		8.96 (-11.23, 29.15)
INV_DROP_LANDING_RFD	20986±10863	30143±20749	**0.001**	-0.520	-9156.65 (-14676.32, -3636.99)
UNINV_LANDING_RFD	32923±30470	52573±36930	**<0.001**	-0.566	-19650.26 (-30516.27, -8784.25)
UNINV_MEAN_TAKEOFF_FORCE	974.6±199.45	1048.8±261.18	0.053		-74.22 (-149.36, 0.93)
UNINV_MEAN_ECCENTRIC_FORCE	1041.6±251.34	1098.8±316.65	0.222		-57.19 (-149.29, 34.91)
UNINV_MEAN_ECC_CON_RATIO	106.88±12.24	104.34±11.82	0.185		2.54 (-1.23, 6.31)
UNINV_PEAK_LANDING_FORCE	1919.7±617.28	2645.2±802.35	**<0.001**	**-0.982**	-725.51 (-956.83, -494.19)
UNINV_PEAK_DROP_FORCE	1698.4±429.2	1917.2±606.91	**0.013**	-0.400	-218.82 (-390, -47.64)
UNINV_PEAK_IMPACT_FORCE	1531±461.14	1716.3±618.25	**0.040**	-0.328	-185.3 (-362.05, -8.54)
UNINV_PEAK_DRIVEOFF_FORCE	1439.9±392.23	1661.6±604.05	**0.010**	-0.415	-221.67 (-388.75, -54.6)
UNINV_PASSIVE_STIFFNESS	12740±6691.4	17883±13078	**0.004**	-0.465	-5143.19 (-8610.39, -1675.99)
UNINV_ACTIVE_STIFFNESS	12920±6492.3	18691±12390	**0.001**	-0.548	-5771.18 (-9067.63, -2474.73)
UNINV_CONCENTRIC_IMPULSE	183.16±40.11	164.59±29.34	**0.001**	0.544	18.57 (7.88, 29.26)
UNINV_FORCE_AT_ZERO_VELOCITY	1360.7±386.38	1599.6±605.09	**0.005**	-0.449	-238.9 (-405.66, -72.13)
UNINV_POSITIVE_IMPULSE	619.72±143.38	529.24±99.21	**<0.001**	0.760	90.48 (53.19, 127.77)
UNINV_ECCENTRIC_IMPULSE	161.87±33.87	146.03±31.03	**0.002**	0.490	15.84 (5.72, 25.96)
UNINV_POSITIVE_TAKEOFF_IMPULSE	337.06±68.35	304.21±55.78	**0.001**	0.536	32.85 (13.65, 52.05)
UNINV_DROP_LANDING_RFD	22686±10322	31125±19141	**0.001**	-0.517	-8438.51 (-13553.83, -3323.18)
LSI_LANDING_RFD	95.26±37.03	105.93±33.96	0.059		-10.67 (-21.75, 0.4)
LSI_MEAN_TAKEOFF_FORCE	89.17±10.94	99.45±10.75	**<0.001**	**-0.946**	-10.29 (-13.69, -6.88)
LSI_MEAN_ECCENTRIC_FORCE	92.23±13.46	97.28±23.72	0.120		-5.05 (-11.44, 1.34)
LSI_MEAN_ECC_CON_RATIO	104.65±19	97.31±18.7	**0.015**	0.388	7.34 (1.42, 13.26)
LSI_PEAK_LANDING_FORCE	92.5±17.36	101.38±20.29	**0.004**	-0.460	-8.88 (-14.92, -2.84)
LSI_PEAK_DROP_FORCE	93.19±12.94	99.74±20.31	**0.022**	-0.367	-6.56 (-12.15, -0.96)
LSI_PEAK_IMPACT_FORCE	93.08±14.11	99.03±24.88	0.081		-5.95 (-12.66, 0.75)
LSI_PEAK_DRIVEOFF_FORCE	92.07±10.26	97.74±10.95	**0.001**	-0.528	-5.67 (-9.03, -2.31)
LSI_PASSIVE_STIFFNESS	99.03±8.24	100.59±9.72	0.288		-1.56 (-4.44, 1.33)
LSI_ACTIVE_STIFFNESS	99.7±1.89	100.11±2.3	0.230		-0.41 (-1.09, 0.26)
LSI_CONCENTRIC_IMPULSE	89.19±10.97	99.72±10.82	**<0.001**	-0.964	-10.53 (-13.95, -7.11)
LSI_FORCE_AT_ZERO_VELOCITY	92.22±11.47	96.68±13.18	**0.027**	-0.354	-4.46 (-8.41, -0.52)
LSI_POSITIVE_IMPULSE	92.35±11.28	98.36±13.51	**0.003**	-0.472	-6.01 (-10, -2.02)
LSI_ECCENTRIC_IMPULSE	92.26±13.68	97.51±24	0.112		-5.25 (-11.72, 1.23)
LSI_POSITIVE_TAKEOFF_IMPULSE	90.76±10.28	98.46±14.9	**<0.001**	-0.577	-7.7 (-11.88, -3.52)
LSI_DROP_LANDING_RFD	95.76±40.08	112.75±78.42	0.109		-16.99 (-37.77, 3.8)

Single leg drop jump

	ACLR n=110	Controls n=123	p value	d	Mean difference (95% CIs)
INV_BEGIN_CONCENTRIC_PHASE	14.53±4.61	13.7±5.67	0.225		0.83 (-0.51, 2.17)
INV_COUNTERMOVEMENT_DEPTH	-16.18±3.3	-14.91±3.3	**0.004**	-0.382	-1.27 (-2.12, -0.41)
INV_BODYMASS_RELATIVE_TAKEOFF_POWER	61.47±9.27	81.23±11.55	**<0.001**	-1.870	-19.76 (-22.48, -17.04)
INV_CONTACT_TIME	0.41±0.09	0.32±0.07	**<0.001**	1.084	0.09 (0.07, 0.11)
INV_FLIGHT_TIME	0.33±0.05	0.39±0.03	**<0.001**	-1.514	-0.06 (-0.07, -0.05)
INV_JUMP_HEIGHT	13.87±3.76	19.13±3.08	**<0.001**	-1.534	-5.26 (-6.15, -4.38)
INV_JUMP_HEIGHT_RELATIVE_LANDING_RFD	2913.6±1580	3204.4±1861.5	0.203		-290.73 (-739.16, 157.71)
INV_JUMP_HEIGHT_RELATIVE_PEAK_LANDING_FORCE	195.94±76.23	170.91±39.86	**0.002**	0.417	25.03 (9.56, 40.5)
INV_IMPULSE_JUMP_HEIGHT	13.91±3.77	19.2±3.08	**<0.001**	-1.539	-5.29 (-6.18, -4.4)
INV_JUMP_HEIGHT_IMP_MOM	13.9±3.78	19.21±3.09	**<0.001**	-1.542	-5.31 (-6.2, -4.42)
INV_LANDING_RFD	39472±26824	60908±37931	**<0.001**	-0.644	-21435.76 (-30008.72, -12862.79)
INV_MEAN_LANDING_ACCELERATION	1.17±1.09	1.23±1.27	0.693		-0.06 (-0.37, 0.24)
INV_MEAN_LANDING_POWER	1129.1±245.72	1219.4±243.33	0.005	-0.368	-90.3 (-153.51, -27.09)
INV_MEAN_LANDING_VELOCITY	-0.19±0.31	-0.29±0.55	0.084		0.1 (-0.01, 0.22)
INV_MEAN_TAKEOFF_ACCELERATION	7.21±1.78	10.92±2.14	**<0.001**	-1.873	-3.72 (-4.23, -3.21)
INV_MEAN_TAKEOFF_FORCE	1302.1±226.86	1633.8±238.93	**<0.001**	-1.417	-331.65 (-391.97, -271.32)
INV_MEAN_ECCENTRIC_FORCE	1449.3±259.85	1710.2±258.02	**<0.001**	-1.005	-260.97 (-327.91, -194.04)
INV_MEAN_ECC_CON_RATIO	111.48±8.06	105.13±9.18	**<0.001**	0.730	6.35 (4.11, 8.59)
INV_MEAN_CONCENTRIC_POWER	3307.3±664.61	4520.4±770.01	**<0.001**	-1.674	-1213.05 (-1399.78, -1026.32)
INV_BODYMASS_RELATIVE_MEAN_CONCENTRIC_POWER	43.33±6.9	57.38±7.89	**<0.001**	-1.882	-14.05 (-15.98, -12.13)
INV_MEAN_TAKEOFF_VELOCITY	1.23±0.13	1.41±0.12	**<0.001**	-1.498	-0.19 (-0.22, -0.15)
INV_PEAK_LANDING_ACCELERATION	23.08±6.14	30.77±7.05	**<0.001**	-1.154	-7.68 (-9.4, -5.97)
INV_PEAK_LANDING_FORCE	2505.2±531.06	3203.1±688.53	**<0.001**	-1.123	-697.91 (-858.02, -537.81)
INV_PEAK_LANDING_POWER	1974.7±433.87	2506.2±611.18	**<0.001**	-0.990	-531.51 (-669.81, -393.21)
INV_PEAK_LANDING_VELOCITY	0.45±0.27	0.45±0.32	0.961		0 (-0.08, 0.08)
INV_PEAK_TAKEOFF_ACCELERATION	14.31±3.97	21.2±5.16	**<0.001**	-1.484	-6.9 (-8.09, -5.7)
INV_PEAK_TAKEOFF_POWER	4703.2±957.86	6403.2±1137.8	**<0.001**	-1.604	-1700.06 (-1973.29, -1426.84)
INV_PEAK_TAKEOFF_VELOCITY	1.88±0.19	2.11±0.15	**<0.001**	-1.370	-0.23 (-0.27, -0.19)
INV_RSI	35.8±12.24	61.96±15.15	**<0.001**	-1.882	-26.16 (-29.74, -22.58)
INV_REACTIVE_STRENGTH_INDEX	0.86±0.21	1.27±0.25	**<0.001**	-1.796	-0.42 (-0.48, -0.36)
INV_START_TO_PEAK_POWER_TIME	0.3±0.09	0.22±0.07	**<0.001**	0.928	0.07 (0.05, 0.09)
INV_WEIGHT_RELATIVE_PEAK_LANDING_FORCE	23.08±6.14	30.77±7.05	**<0.001**	-1.154	-7.68 (-9.4, -5.97)
INV_PEAK_DROP_FORCE	2161.8±469.54	2618.4±482.17	**<0.001**	-0.956	-456.6 (-579.74, -333.46)
INV_CONTACT_VELOCITY	-1.48±0.15	-1.59±0.18	**<0.001**	0.641	0.11 (0.06, 0.15)
INV_DROP_HEIGHT	11.36±2.21	13.12±3.08	**<0.001**	-0.652	-1.77 (-2.47, -1.07)
INV_EFFECTIVE_DROP	11.36±2.21	13.12±3.08	**<0.001**	-0.652	-1.77 (-2.47, -1.07)
INV_DROP_LANDING	14.36±4.61	13.56±5.66	0.243		0.8 (-0.55, 2.14)
INV_TAKEOFF_VELOCITY	1.63±0.23	1.93±0.16	**<0.001**	-1.523	-0.3 (-0.35, -0.25)
INV_PEAK_IMPACT_FORCE	1979.7±551.78	2256.7±685.59	**0.001**	-0.441	-277.01 (-438.87, -115.14)
INV_CONTACT_TROUGH	1555.8±454.76	1936±619.43	**<0.001**	-0.691	-380.11 (-521.78, -238.44)
INV_PEAK_DRIVEOFF_FORCE	1900.8±415.75	2461.4±476.94	**<0.001**	-1.244	-560.62 (-676.74, -444.5)
INV_PASSIVE_STIFFNESS	12999±5004.7	16455±8185.8	**<0.001**	-0.501	-3455.4 (-5231.91, -1678.9)
INV_ACTIVE_STIFFNESS	12501±4281.6	17735±6103.9	**<0.001**	-0.980	-5234.12 (-6610.26, -3857.99)
INV_PASSIVE_STIFFNESS_INDEX	1.93±0.67	2.74±1.4	**<0.001**	-0.717	-0.8 (-1.09, -0.52)
INV_ACTIVE_STIFFNESS_INDEX	1.85±0.59	2.92±1.03	**<0.001**	-1.248	-1.07 (-1.29, -0.85)
INV_CONCENTRIC_IMPULSE	124.82±23.72	152.55±20.98	**<0.001**	-1.239	-27.74 (-33.51, -21.97)
INV_FORCE_AT_ZERO_VELOCITY	1782.7±431.62	2387±512.66	**<0.001**	-1.265	-604.33 (-727.44, -481.22)
INV_POSITIVE_IMPULSE	433.32±80.65	492.93±67.42	**<0.001**	-0.803	-59.6 (-78.72, -40.48)
INV_ECCENTRIC_IMPULSE	112.83±19.67	124.57±19.07	**<0.001**	-0.605	-11.74 (-16.75, -6.74)
INV_JUMP_HEIGHT_INCHES	5.46±1.48	7.53±1.21	**<0.001**	-1.534	-2.07 (-2.42, -1.72)
INV_JUMP_HEIGHT_INCHES_IMP_MOM	5.47±1.49	7.56±1.21	**<0.001**	-1.542	-2.09 (-2.44, -1.74)
INV_POSITIVE_TAKEOFF_IMPULSE	265.63±45.28	298.81±38.01	**<0.001**	-0.795	-33.18 (-43.94, -22.42)
INV_DROP_LANDING_RFD	31147±17593	32258±25328	0.701		-1111 (-6804.32, 4582.32)

UNINV_BEGIN_CONCENTRIC_PHASE	15±6.64	14.51±6.24	0.563		0.49 (-1.17, 2.15)
UNINV_COUNTERMOVEMENT_DEPTH	-17.14±3.49	-14.96±3.21	**<0.001**	-0.648	-2.18 (-3.04, -1.31)
UNINV_BODYMASS_RELATIVE_TAKEOFF_POWER	67.83±10.6	80.39±10.82	**<0.001**	-1.169	-12.57 (-15.34, -9.8)
UNINV_CONTACT_TIME	0.38±0.08	0.32±0.07	**<0.001**	0.804	0.06 (0.04, 0.08)
UNINV_FLIGHT_TIME	0.36±0.05	0.39±0.03	**<0.001**	-0.782	-0.03 (-0.04, -0.02)
UNINV_JUMP_HEIGHT	16.31±3.94	18.9±2.81	**<0.001**	-0.762	-2.59 (-3.47, -1.72)
UNINV_JUMP_HEIGHT_RELATIVE_LANDING_RFD	2493.3±1327.2	3360.4±2274.7	**0.001**	-0.458	-867.15 (-1355.26, -379.03)
UNINV_JUMP_HEIGHT_RELATIVE_PEAK_LANDING_FORCE	166.1±51.3	174.75±38.66	0.145		-8.64 (-20.3, 3.01)
UNINV_IMPULSE_JUMP_HEIGHT	16.35±3.95	18.95±2.82	**<0.001**	-0.764	-2.6 (-3.48, -1.73)
UNINV_JUMP_HEIGHT_IMP_MOM	16.34±3.95	18.96±2.82	**<0.001**	-0.766	-2.61 (-3.49, -1.74)
UNINV_LANDING_RFD	40860±32339	63497±45788	**<0.001**	-0.564	-22637.15 (-32981.89, -12292.41)
UNINV_MEAN_LANDING_ACCELERATION	1.39±1.15	1.14±1.29	0.125		0.25 (-0.07, 0.56)
UNINV_MEAN_LANDING_POWER	1175.7±270.02	1214.5±272.27	0.277		-38.8 (-108.93, 31.32)
UNINV_MEAN_LANDING_VELOCITY	-0.2±0.3	-0.33±0.52	**0.021**	0.304	0.13 (0.02, 0.24)
UNINV_MEAN_TAKEOFF_ACCELERATION	8.46±2.04	10.75±1.99	**<0.001**	-1.131	-2.29 (-2.81, -1.77)
UNINV_MEAN_TAKEOFF_FORCE	1397.6±245.72	1618.4±222.18	**<0.001**	-0.942	-220.79 (-281.18, -160.39)
UNINV_MEAN_ECCENTRIC_FORCE	1498.4±260.08	1718.8±269.77	**<0.001**	-0.828	-220.37 (-288.95, -151.79)
UNINV_MEAN_ECC_CON_RATIO	107.55±7.76	106.29±8.07	0.226		1.26 (-0.79, 3.31)
UNINV_MEAN_CONCENTRIC_POWER	3719.3±699.61	4491.5±717.98	**<0.001**	-1.085	-772.16 (-955.57, -588.74)
UNINV_BODYMASS_RELATIVE_MEAN_CONCENTRIC_POWER	48.77±7.5	57.04±7.2	**<0.001**	-1.123	-8.27 (-10.17, -6.37)
UNINV_MEAN_TAKEOFF_VELOCITY	1.3±0.13	1.4±0.11	**<0.001**	-0.861	-0.1 (-0.13, -0.07)
UNINV_PEAK_LANDING_ACCELERATION	23.98±6.27	31.41±7.49	**<0.001**	-1.066	-7.43 (-9.22, -5.63)
UNINV_PEAK_LANDING_FORCE	2571.1±545.91	3245.3±675.5	**<0.001**	-1.088	-674.19 (-833.91, -514.46)
UNINV_PEAK_LANDING_POWER	2108.2±508.02	2574.9±676.61	**<0.001**	-0.771	-466.7 (-622.6, -310.8)
UNINV_PEAK_LANDING_VELOCITY	0.48±0.24	0.45±0.36	0.449		0.03 (-0.05, 0.11)
UNINV_PEAK_TAKEOFF_ACCELERATION	16.14±4.49	20.98±5.31	**<0.001**	-0.975	-4.84 (-6.11, -3.56)
UNINV_PEAK_TAKEOFF_POWER	5182.3±1028.8	6333.5±1075.7	**<0.001**	-1.089	-1151.18 (-1423.65, -878.71)
UNINV_PEAK_TAKEOFF_VELOCITY	1.98±0.19	2.09±0.14	**<0.001**	-0.686	-0.11 (-0.16, -0.07)
UNINV_RSI	44.65±14.68	60.66±13.45	**<0.001**	-1.136	-16.02 (-19.65, -12.38)
UNINV_REACTIVE_STRENGTH_INDEX	0.99±0.24	1.26±0.24	**<0.001**	-1.140	-0.27 (-0.33, -0.21)
UNINV_START_TO_PEAK_POWER_TIME	0.28±0.08	0.22±0.07	**<0.001**	0.747	0.06 (0.04, 0.08)
UNINV_WEIGHT_RELATIVE_PEAK_LANDING_FORCE	23.98±6.27	31.41±7.49	**<0.001**	-1.066	-7.43 (-9.22, -5.63)
UNINV_PEAK_DROP_FORCE	2194.7±486.03	2602.9±497.51	**<0.001**	-0.827	-408.21 (-535.46, -280.97)
UNINV_CONTACT_VELOCITY	-1.55±0.15	-1.61±0.18	**0.023**	0.300	0.05 (0.01, 0.1)
UNINV_DROP_HEIGHT	12.46±2.44	13.35±3.1	**0.017**	-0.314	-0.89 (-1.61, -0.16)
UNINV_EFFECTIVE_DROP	12.46±2.44	13.35±3.1	**0.017**	-0.314	-0.89 (-1.61, -0.16)
UNINV_DROP_LANDING	14.83±6.64	14.37±6.24	0.584		0.46 (-1.2, 2.13)
UNINV_TAKEOFF_VELOCITY	1.78±0.22	1.92±0.14	**<0.001**	-0.786	-0.15 (-0.19, -0.1)
UNINV_PEAK_IMPACT_FORCE	1921.2±570.76	2208±709.1	**0.001**	-0.442	-286.85 (-454.28, -119.43)
UNINV_CONTACT_TROUGH	1604.4±457.18	1883.7±620.24	**<0.001**	-0.507	-279.26 (-421.3, -137.22)
UNINV_PEAK_DRIVEOFF_FORCE	2028.3±440.88	2449.4±471.94	**<0.001**	-0.917	-421.08 (-539.38, -302.77)
UNINV_PASSIVE_STIFFNESS	11901±4808	15823±7132.3	**<0.001**	-0.636	-3922.41 (-5511.52, -2333.29)
UNINV_ACTIVE_STIFFNESS	12678±4625.3	17590±6231.8	**<0.001**	-0.885	-4912.12 (-6342.51, -3481.73)
UNINV_PASSIVE_STIFFNESS_INDEX	1.95±0.7	2.68±1.29	**<0.001**	-0.693	-0.74 (-1.01, -0.46)
UNINV_ACTIVE_STIFFNESS_INDEX	2.06±0.69	2.94±1.01	**<0.001**	-1.012	-0.89 (-1.11, -0.66)
UNINV_CONCENTRIC_IMPULSE	135.85±24.88	151.57±19.78	**<0.001**	-0.701	-15.71 (-21.49, -9.94)
UNINV_FORCE_AT_ZERO_VELOCITY	1943.5±442.06	2368.1±508.79	**<0.001**	-0.884	-424.57 (-548.28, -300.86)
UNINV_POSITIVE_IMPULSE	459.25±80.86	491.38±67	**0.001**	-0.434	-32.13 (-51.23, -13.03)
UNINV_ECCENTRIC_IMPULSE	118.13±20.03	125.76±19.75	**0.004**	-0.383	-7.63 (-12.77, -2.49)
UNINV_JUMP_HEIGHT_INCHES	6.42±1.55	7.44±1.11	**<0.001**	-0.762	-1.02 (-1.37, -0.68)
UNINV_JUMP_HEIGHT_INCHES_IMP_MOM	6.44±1.56	7.46±1.11	**<0.001**	-0.766	-1.03 (-1.38, -0.68)
UNINV_POSITIVE_TAKEOFF_IMPULSE	279.12±45.84	298.94±37.79	**<0.001**	-0.473	-19.82 (-30.63, -9.02)
UNINV_DROP_LANDING_RFD	26966±14348	33552±20075	**0.005**	-0.373	-6586 (-11138.23, -2033.77)
LSI_BEGIN_CONCENTRIC_PHASE	106.84±41	106.87±60.53	0.996		-0.03 (-13.54, 13.47)
LSI_COUNTERMOVEMENT_DEPTH	95.36±13.53	100.24±12.42	**0.005**	-0.375	-4.88 (-8.23, -1.53)
LSI_BODYMASS_RELATIVE_TAKEOFF_POWER	91.15±9.01	101.33±8.84	**<0.001**	-1.138	-10.18 (-12.49, -7.88)
LSI_CONTACT_TIME	106.45±12.99	99.86±10.06	**<0.001**	0.570	6.6 (3.61, 9.58)
LSI_FLIGHT_TIME	92.01±6.48	100.7±6.4	**<0.001**	-1.347	-8.7 (-10.36, -7.03)

LSI_JUMP_HEIGHT	85.08±11.83	101.81±12.83	**<0.001**	-1.348	-16.73 (-19.93, -13.53)
LSI_JUMP_HEIGHT_RELATIVE_LANDING_RFD	118.06±29.51	100.4±24.44	**<0.001**	0.653	17.66 (10.69, 24.63)
LSI_JUMP_HEIGHT_RELATIVE_PEAK_LANDING_FORCE	117.35±19.2	98.75±16.03	**<0.001**	1.054	18.6 (14.05, 23.15)
LSI_IMPULSE_JUMP_HEIGHT	85.11±11.81	101.88±12.83	**<0.001**	-1.352	-16.77 (-19.97, -13.57)
LSI_JUMP_HEIGHT_IMP_MOM	85.11±11.82	101.93±12.86	**<0.001**	-1.354	-16.82 (-20.02, -13.62)
LSI_LANDING_RFD	99.36±25.85	102.11±26.39	0.422		-2.76 (-9.51, 4)
LSI_MEAN_LANDING_ACCELERATION	37.26±465.82	100.46±829.7	0.481		-63.2 (-239.69, 113.3)
LSI_MEAN_LANDING_POWER	97.81±18.33	104.43±29.23	**0.042**	-0.267	-6.62 (-13.01, -0.24)
LSI_MEAN_LANDING_VELOCITY	139.53±383.43	212.26±572.95	0.262		-72.73 (-200.12, 54.66)
LSI_MEAN_TAKEOFF_ACCELERATION	86.08±13.94	102.18±12.81	**<0.001**	-1.202	-16.1 (-19.55, -12.65)
LSI_MEAN_TAKEOFF_FORCE	93.44±6.45	100.99±6.52	**<0.001**	-1.161	-7.56 (-9.24, -5.88)
LSI_MEAN_ECCENTRIC_FORCE	96.82±6.48	99.86±6.83	**0.001**	-0.454	-3.04 (-4.76, -1.31)
LSI_MEAN_ECC_CON_RATIO	103.86±6.57	99.06±6.84	**<0.001**	0.711	4.79 (3.06, 6.53)
LSI_MEAN_CONCENTRIC_POWER	89.18±9.09	100.91±9.53	**<0.001**	-1.254	-11.73 (-14.14, -9.32)
LSI_BODYMASS_RELATIVE_MEAN_CONCENTRIC_POWER	89.18±9.09	100.91±9.53	**<0.001**	-1.255	-11.73 (-14.15, -9.32)
LSI_MEAN_TAKEOFF_VELOCITY	94.36±6.14	100.66±6.33	**<0.001**	-1.006	-6.3 (-7.91, -4.68)
LSI_PEAK_LANDING_ACCELERATION	97.73±16.2	99.73±19.03	0.393		-1.99 (-6.58, 2.59)
LSI_PEAK_LANDING_FORCE	98.03±10.93	99.46±13.89	0.388		-1.43 (-4.68, 1.82)
LSI_PEAK_LANDING_POWER	94.99±13.95	99.85±21.27	**0.043**	-0.266	-4.86 (-9.56, -0.16)
LSI_PEAK_LANDING_VELOCITY	100.54±73.25	90.81±98.42	0.397		9.73 (-12.88, 32.34)
LSI_PEAK_TAKEOFF_ACCELERATION	90.33±16.75	102.16±13.98	**<0.001**	-0.768	-11.83 (-15.8, -7.86)
LSI_PEAK_TAKEOFF_POWER	91.15±9.01	101.33±8.84	**<0.001**	-1.138	-10.18 (-12.49, -7.87)
LSI_PEAK_TAKEOFF_VELOCITY	94.91±4.93	100.67±5.35	**<0.001**	-1.114	-5.76 (-7.09, -4.43)
LSI_RSI	81.23±16.13	102.99±16.81	**<0.001**	-1.314	-21.75 (-26.02, -17.49)
LSI_REACTIVE_STRENGTH_INDEX	87.72±13.09	101.83±12.01	**<0.001**	-1.122	-14.11 (-17.35, -10.87)
LSI_START_TO_PEAK_POWER_TIME	106.55±18.09	100.61±13.58	**0.005**	0.374	5.95 (1.85, 10.05)
LSI_WEIGHT_RELATIVE_PEAK_LANDING_FORCE	97.73±16.2	99.73±19.03	0.393		-1.99 (-6.58, 2.59)
LSI_PEAK_DROP_FORCE	99.15±11.34	101.07±9.1	0.154		-1.92 (-4.56, 0.73)
LSI_CONTACT_VELOCITY	95.67±7.04	99.48±8.38	**<0.001**	-0.488	-3.81 (-5.82, -1.8)
LSI_DROP_HEIGHT	92.05±13.54	99.65±16.94	**<0.001**	-0.491	-7.6 (-11.59, -3.61)
LSI_EFFECTIVE_DROP	92.05±13.54	99.65±16.94	**<0.001**	-0.491	-7.6 (-11.59, -3.61)
LSI_DROP_LANDING	106.99±41.56	107.1±61.4	0.988		-0.11 (-13.8, 13.59)
LSI_TAKEOFF_VELOCITY	92.02±6.47	100.77±6.41	**<0.001**	-1.355	-8.75 (-10.42, -7.09)
LSI_PEAK_IMPACT_FORCE	110.73±51.56	111.81±55.73	0.879		-1.08 (-14.99, 12.83)
LSI_CONTACT_TROUGH	107±62.69	115.9±73.9	0.325		-8.9 (-26.7, 8.9)
LSI_PEAK_DRIVEOFF_FORCE	94.31±10.33	100.74±8.36	**<0.001**	-0.686	-6.43 (-8.85, -4.01)
LSI_PASSIVE_STIFFNESS	119.09±60.13	113.47±56.72	0.464		5.61 (-9.47, 20.7)
LSI_ACTIVE_STIFFNESS	101.27±20.43	102.28±16.98	0.681		-1.01 (-5.84, 3.82)
LSI_PASSIVE_STIFFNESS_INDEX	109.08±57.7	113.59±64.04	0.574		-4.51 (-20.32, 11.29)
LSI_ACTIVE_STIFFNESS_INDEX	92.37±20.27	100.86±18.72	**0.001**	-0.435	-8.49 (-13.52, -3.46)
LSI_CONCENTRIC_IMPULSE	91.98±6.49	100.76±6.44	**<0.001**	-1.354	-8.78 (-10.45, -7.11)
LSI_FORCE_AT_ZERO_VELOCITY	92.12±11.18	101.36±10.89	**<0.001**	-0.835	-9.24 (-12.09, -6.38)
LSI_POSITIVE_IMPULSE	94.35±5.85	100.62±7.72	**<0.001**	-0.904	-6.26 (-8.05, -4.48)
LSI_ECCENTRIC_IMPULSE	95.7±7.12	99.47±8.43	**<0.001**	-0.479	-3.77 (-5.8, -1.74)
LSI_JUMP_HEIGHT_INCHES	85.08±11.83	101.81±12.83	**<0.001**	-1.348	-16.73 (-19.93, -13.53)
LSI_JUMP_HEIGHT_INCHES_IMP_MOM	85.11±11.82	101.93±12.86	**<0.001**	-1.354	-16.82 (-20.02, -13.62)
LSI_POSITIVE_TAKEOFF_IMPULSE	95.17±4.26	100.07±4.79	**<0.001**	-1.073	-4.9 (-6.07, -3.72)
LSI_DROP_LANDING_RFD	123.52±50.42	101.09±43.15	**<0.001**	0.479	22.44 (10.36, 34.52)